FRA-76-13

REPORT NO. FRA-OR&D-76-293

COMPUTATIONAL METHODS TO PREDICT RAILCAR RESPONSE TO TRACK CROSS-LEVEL VARIATIONS

B. E. Platin
J. J. Beaman
J. K. Hedrick
D. N. Wormley

Massachusetts Institute of Technology
Department of Mechanical Engineering
Cambridge MA 02139

SEPTEMBER 1976
FINAL REPORT

Prepared for

U.S. DEPARTMENT OF TRANSPORTATION
FEDERAL RAILROAD ADMINISTRATION
Research and Development
Office of Rail Safety Research
Washington DC 20590

Technical Report Documentation Page

1. Report No.: FRA-OR&D-76-293

2. Government Accession No.:

3. Recipient's Catalog No.:

4. Title and Subtitle: COMPUTATIONAL METHODS TO PREDICT RAILCAR RESPONSE TO TRACK CROSS-LEVEL VARIATIONS

5. Report Date: September 1976

6. Performing Organization Code:

8. Performing Organization Report No.: DOT-TSC-FRA-76-13

7. Author(s): B.E. Platin, J.J. Beaman, J.K. Hedrick and D.N. Wormley

9. Performing Organization Name and Address:
Massachusetts Institute of Technology*
Department of Mechanical Engineering
Cambridge MA 02139

10. Work Unit No. (TRAIS): RR619/R6365

11. Contract or Grant No.: DOT-TS-11201

12. Sponsoring Agency Name and Address:
U.S. Department of Transportation
Federal Railroad Administration
Research and Development
Office of Rail Safety Research
Washington DC 20590

13. Type of Report and Period Covered: Final Report, September 1975 - May 1976

14. Sponsoring Agency Code:

15. Supplementary Notes:
*Under contract to: U.S. Department of Transportation
Transportation Systems Center
Kendall Square
Cambridge MA 02142

16. Abstract

The rocking response of railroad freight cars to track cross-level variations is studied using (1) a reduced complexity digital simulation model, and (2) a quasi-linear describing function analysis. The reduced complexity digital simulation model employs a rail truck model that neglects the high-frequency dynamics of the bolster and wheelset masses, yet includes kinematic center plate, side bearings, and wheelset nonlinear effects. This model has computation-time requirements that are less than one eighth those of more detailed computer simulation models and agrees within 15% percent for the prediction of roll angle, side bearing force, center plate force and wheel force at maximum roll angle response with the more detailed models

A study of quasi-linear describing function techniques to compute the steady-state response of freight cars to equivalent sinusoidal cross-level track variations has demonstrated the feasibility of the technique for the types of nonlinearities important in car response. This technique, which computes steady-state response from a set of nonlinear algebraic equations rather than by numerical integration, is effective for parametric studies in which a series of the responses is required as a parameter is varied incrementally since once the solution is obtained for one set of parameter values, additional responses for an incremental change in the parameter are obtained efficiently.

17. Key Words: Track Train Dynamics, Rail Car Rock and Roll, Computational Methods

18. Distribution Statement: DOCUMENT IS AVAILABLE TO THE U.S. PUBLIC THROUGH THE NATIONAL TECHNICAL INFORMATION SERVICE, SPRINGFIELD, VIRGINIA 22161

19. Security Classif. (of this report)	20. Security Classif. (of this page)	21. No. of Pages	22. Price
Unclassified	Unclassified	86	

PREFACE

The work described here was conducted in support of the Improved Track Structures Research Program of the Office of Rail Safety Research of the Federal Railroad Administration as a limited-scope engineering-data service type of contract. Under this program, the Transportation Systems Center is conducting analytical and experimental studies of the relations between track-geometry variations and railcar safety.

The investigators wish to acknowledge the fruitful technical discussions held during the course of the work with Herbert Weinstock of the U.S. Department of Transportation, Transportation Systems Center. We are also grateful to Derek Rowell from the M.I.T. Department of Mechanical Engineering who assisted in computer implementation of the describing function analysis.

METRIC CONVERSION FACTORS

Approximate Conversions to Metric Measures

Symbol	When You Know	Multiply by	To Find	Symbol
		LENGTH		
in	inches	2.5	centimeters	cm
ft	feet	30	centimeters	cm
yd	yards	0.9	meters	m
mi	miles	1.6	kilometers	km
		AREA		
in^2	square inches	6.5	square centimeters	cm^2
ft^2	square feet	0.09	square meters	m^2
yd^2	square yards	0.8	square meters	m^2
mi^2	square miles	2.6	square kilometers	km^2
	acres	0.4	hectares	ha
		MASS (weight)		
oz	ounces	28	grams	g
lb	pounds	0.45	kilograms	kg
	short tons (2000 lb)	0.9	tonnes	t
		VOLUME		
tsp	teaspoons	5	milliliters	ml
Tbsp	tablespoons	15	milliliters	ml
fl oz	fluid ounces	30	milliliters	ml
c	cups	0.24	liters	l
pt	pints	0.47	liters	l
qt	quarts	0.95	liters	l
gal	gallons	3.8	liters	l
ft^3	cubic feet	0.03	cubic meters	m^3
yd^3	cubic yards	0.76	cubic meters	m^3
		TEMPERATURE (exact)		
°F	Fahrenheit temperature	5/9 (after subtracting 32)	Celsius temperature	°C

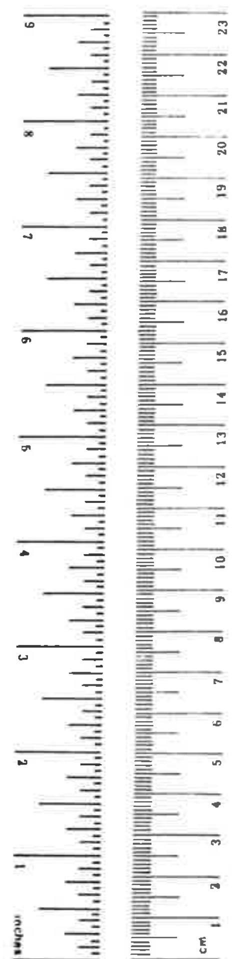

Approximate Conversions from Metric Measures

Symbol	When You Know	Multiply by	To Find	Symbol
		LENGTH		
mm	millimeters	0.04	inches	in
cm	centimeters	0.4	inches	in
m	meters	3.3	feet	ft
m	meters	1.1	yards	yd
km	kilometers	0.6	miles	mi
		AREA		
cm^2	square centimeters	0.16	square inches	in^2
m^2	square meters	1.2	square yards	yd^2
km^2	square kilometers	0.4	square miles	mi^2
ha	hectares (10,000 m^2)	2.5	acres	
		MASS (weight)		
g	grams	0.035	ounces	oz
kg	kilograms	2.2	pounds	lb
t	tonnes (1000 kg)	1.1	short tons	
		VOLUME		
ml	milliliters	0.03	fluid ounces	fl oz
l	liters	2.1	pints	pt
l	liters	1.06	quarts	qt
l	liters	0.26	gallons	gal
m^3	cubic meters	35	cubic feet	ft^3
m^3	cubic meters	1.3	cubic yards	yd^3
		TEMPERATURE (exact)		
°C	Celsius temperature	9/5 (then add 32)	Fahrenheit temperature	°F

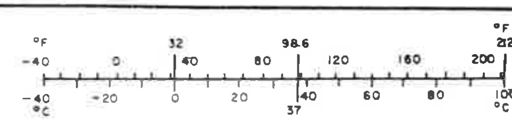

CONTENTS

ILLUSTRATIONS

ILLUSTRATIONS (Concl'd)

TABLES

1. INTRODUCTION

Freight car response to cross level track disturbances directly influences freight car operation. Under low speed (10-20 mph) operating conditions freight car response to track cross level variations can result in severe car rocking with wheel-track dynamic forces two-three times nominal static force levels, high car body-bolster dynamic forces approaching 2.5 times the nominal static force levels and large rocking angles approaching $\pm$ 5-7°. These large dynamic force levels which occur in severe rocking conditions degrade both track and equipment performance over a period of time and thus directly influence car operation and safety.

In the last decade the introduction of high center-of-gravity cars with car truck center-to-center lengths equal to track length (39 feet) and the necessity to operate on track with significant cross level variation (1/2 inch or greater) has led to increased interest in the rocking problem [1-3]. Work at the AAR [4 and 5], Illinois Institute of Technology [6], Wyle Laboratories [7], Stucki [8], and MIT [9 and 10], has led to development of analog and digital computer simulation programs to predict the rocking response of freight cars to cross level track variations. The computer programs developed represent a wide spectrum of model detail and complexity and correspondingly require varying amounts of computer time and cost to run. The most widely disseminated program has been developed by AAR. Their work resulted in preparation and documentation of a digital program for computation of car response. The AAR program has been developed to a high level of detail and includes flexible car body effects, the effects of bolster and wheelset masses, as well as nonlinear suspension springs and damping. The program has been useful to a number of organizations in car response studies.

The objective of the present study is to evaluate the use of reduced complexity freight car digital simulation models and quasi-linearization techniques for computation of car rocking response. The principal motivation is to develop a car response model with adequate accuracy for general parametric studies which has significantly reduced computation time requirements in comparison to the more detailed models cited above. The first part of the study is directed to evaluation of a freight car response computation model which uses a relatively simple representation of the truck in which the truck bolster and wheelset inertial forces are neglected while the suspension nonlinear stiffness and damping effects are considered. Because the high frequency* effects associated with the bolster and wheelset inertias reacting against high stiffness springs (gib stop and track stiffness) are neglected in this model, its intergration step size interval is twenty times that required in more complex truck models, and the total computation time requirement approaches one eighth that of more complex models.

The second part of the study consists of an evaluation of quasi-linearization techniques to determine freight car steady-state response to a sinusoidal model of track cross level irregularities. Because these techniques allow incorporation of the principal nonlinear

*These frequencies for typical 70 and 100 ton cars are in the 200-1000 hertz range.

effects in freight car response in a quasi-linear manner, yet are based upon efficient linear computation techniques, they merit evaluation for use in parametric studies of freight car response.

The study of digital simulation and quasi-linearization techniques described in this report has been of limited scope and cost, and has focused on accuracy and time requirements of computation techniques for freight car response. Parametric response data to show the influence of nonlinearities on response characteristics has been developed. However, the limited scope of the study has precluded extensive documentation of the detailed derivation of the simulation and quasi-linearization model equations and of the computer programs in this report. This documentation will be completed and presented in M.I.T. theses to be published in January 1977.

2. SIMULATION MODEL

2.1 Car Rocking Kinematic Behavior

A section view of a freight car on a track with cross level variation is sketched in Fig. 1. The primary elements in the car include the car body and front and rear trucks each of which contains a bolster, two side frames, two wheelsets and two suspension spring sets. As the car travels down the track, cross level track variations result in a vertical displacement of the right wheels with respect to the left wheels. This input displacement is transmitted through the suspension springs to the bolster and in turn through the center plate and side bearings to the car body and results in car rocking response. For reference in further discussion, three levels of rocking response may be identified in terms of the kinematics or rocking.

a) Light Rocking in which the wheels remain on and follow the tracks and the car body remains on the center plate with no side bearing contact.

b) Moderate Rocking in which the car body rocks to contact the side bearings but remains in contact with the center plate. As the car body rocks onto the side bearings the bolster can move laterally into the gib stops.

c) Severe Rocking in which the car body rocks out of contact with the center plate onto the side bearings and drives the bolster into the gib stops. In this mode significant wheel lift occurs.

To predict the motion of a freight car which is valid for the three kinematic modes of motion described requires formulation of a nonlinear model. Essential to this model are the effects of:

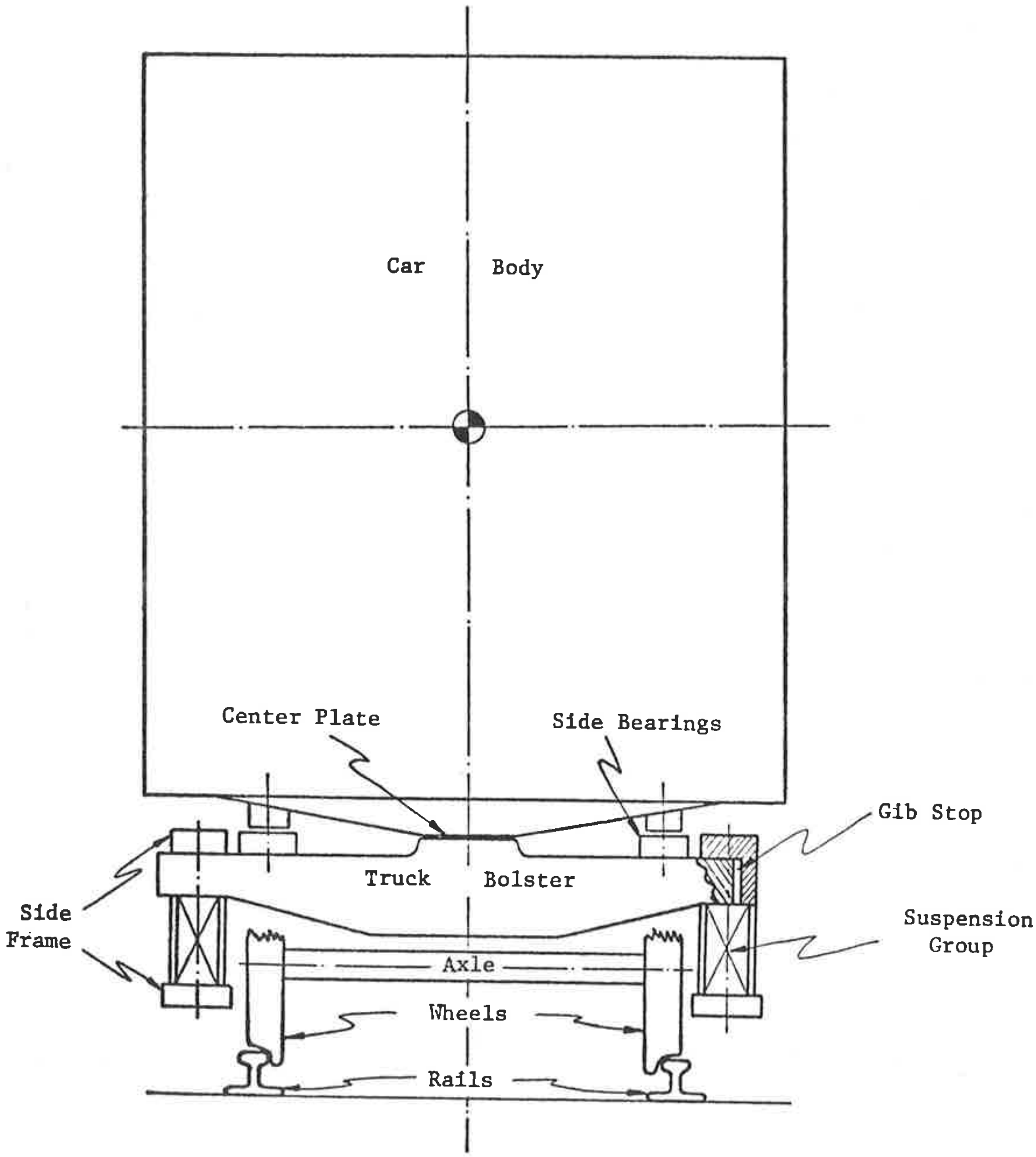

FIGURE 1. A TYPICAL FREIGHT CAR AND TRUCK IN TRANSVERSE PLANE

1) Car body rocking on and separation from the center plate,

2) Side bearing contact,

3) Wheel lift,

4) Suspension group non-linear stiffness due to spring bottoming in vertical motion and gib stop contact in lateral motion,

5) Suspension group coulomb damping for vertical and lateral motion.

These effects have been included with various modeling techniques in models cited in [4-8]. The treatment of these effects in this study is described in the following section.

2.2 Digital Simulation Model

Full and half car body digital simulation models have been developed to determine freight car response. In the models the track has been represented as a rectified sine wave displacement with amplitude:

$$y_r = A\left|\sin\left(\frac{\pi V t}{\ell_r}\right)\right| , \qquad (1)$$

$$y_\ell = A\left|\sin\left(\frac{\pi V t}{\ell_r} + \frac{\pi}{2}\right)\right| . \qquad (2)$$

Where:
- y_r = right track displacement
- y_ℓ = left track displacement
- A = amplitude of cross level variation
- V = car forward velocity
- t = time
- ℓ_r = rail length.

Because the track is staggered, the left track displacement if 90° out of phase with the right track. The effective frequency of the sine wave model is a function of velocity V and track length ℓ_r. In this model the effects of track compliance are neglected.

The car is represented by a model of the car body and models of each track. For clarity in the paragraphs below only a half car body model is described, since the extension to the full car body model is straightforward.

The half car body model is sketched in Figure 2. The car body has vertical, lateral and rotational degrees of freedom and is assumed to travel down the track at velocity, V. The half car body vertical motion equation is:

$$M\ddot{z} = F_{sr} + F_{cr} + F_{c\ell} + F_{s\ell} - Mg \,, \tag{3}$$

where: M = mass of half car body

$\ddot{z}$ = vertical acceleration of car body

$F_{s\ell}, F_{c\ell}, F_{cr}, F_{sr}$ = vertical forces respectively from left side bearing, left center plate corner, right center plate corner, and right side bearing

g = gravitational acceleration.

Each of the forces F_{sr}, $F_{s\ell}$, $F_{c\ell}$, F_{cr} is determined by the truck bolster-car body interface and can be zero when no contact occurs between the car body and a support point. These forces cannot be negative.

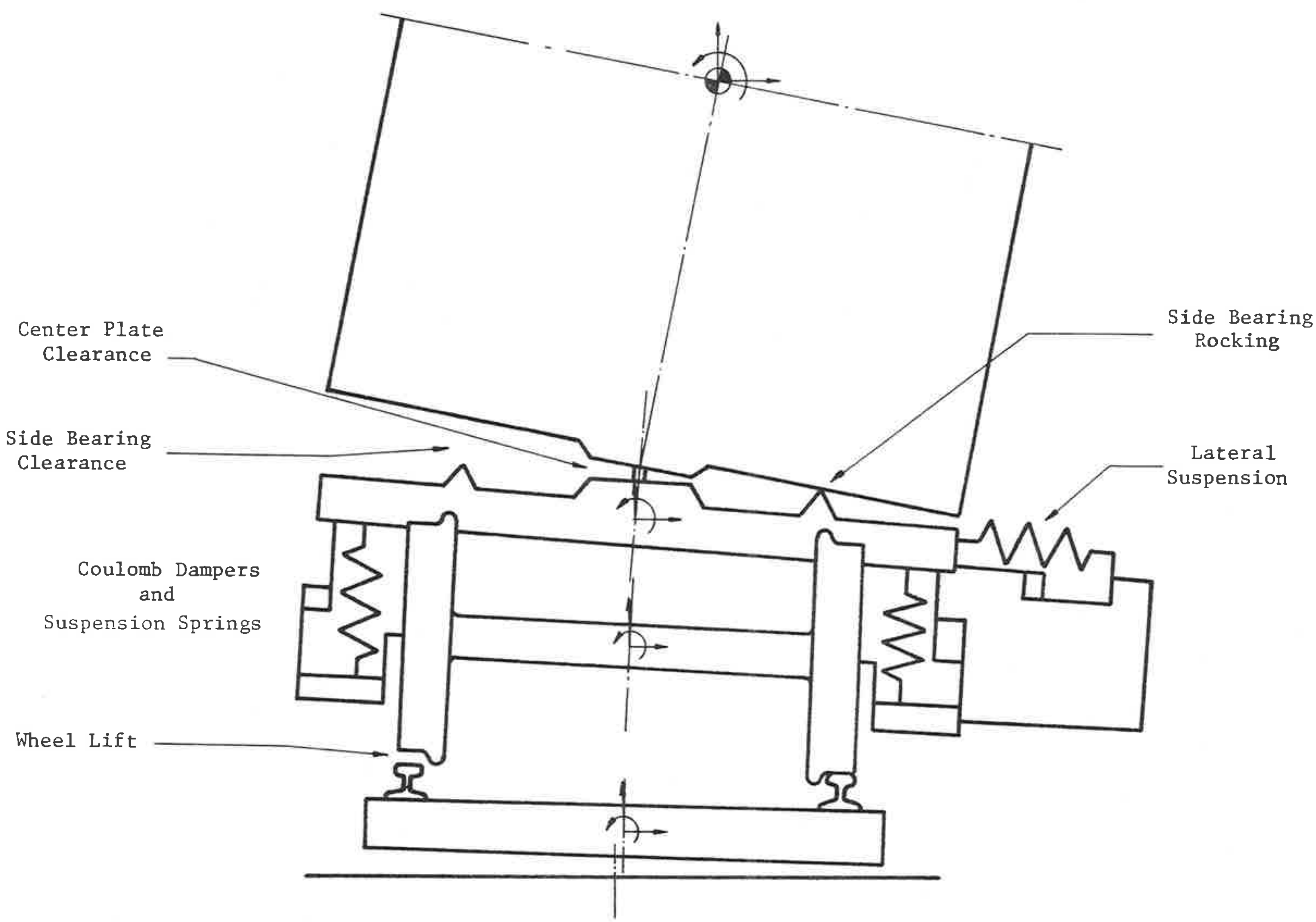

FIGURE 2. RAILROAD FREIGHT CAR SIMULATION MODEL

The lateral motion equation is:

$$M \ddot{y} = F_h \tag{4}$$

where: $\ddot{y}$ = lateral acceleration of car body

F_h = lateral force between the car body and bolster.

The lateral force between the car body and bolster is assumed to be transmitted by the center pin and is determined by the truck bolster, car body relative lateral position.

The rotational equation of motion is

$$\begin{aligned} I \ddot{\theta} &= a_s(F_{sr}-F_{s\ell}) + a_c(F_{cr}-F_{c\ell}) + bF_h \\ &+ b(F_{sr} + F_{cr} + F_{c\ell} + F_{s\ell})\theta , \end{aligned} \tag{5}$$

where: I = half car body roll moment of inertia

$\ddot{\theta}$ = rotational acceleration of car body

a_c = center plate radius

a_s = distance from truck center to side bearing

b = car body c.g. height above center plate.

At any point in time the accelerations $\ddot{z}$, $\ddot{y}$ and $\ddot{\theta}$ may be determined directly from the bolster-car body contact forces as summarized in (3), (4) and (5), and integrated to yield the car body velocity and position in space. Four of the eight possible positions of the car body relative to the truck bolster are shown in Figure 3 with the three left hand positions which are symmetric with respect to those shown and the position of no point of contact not shown. For each car-

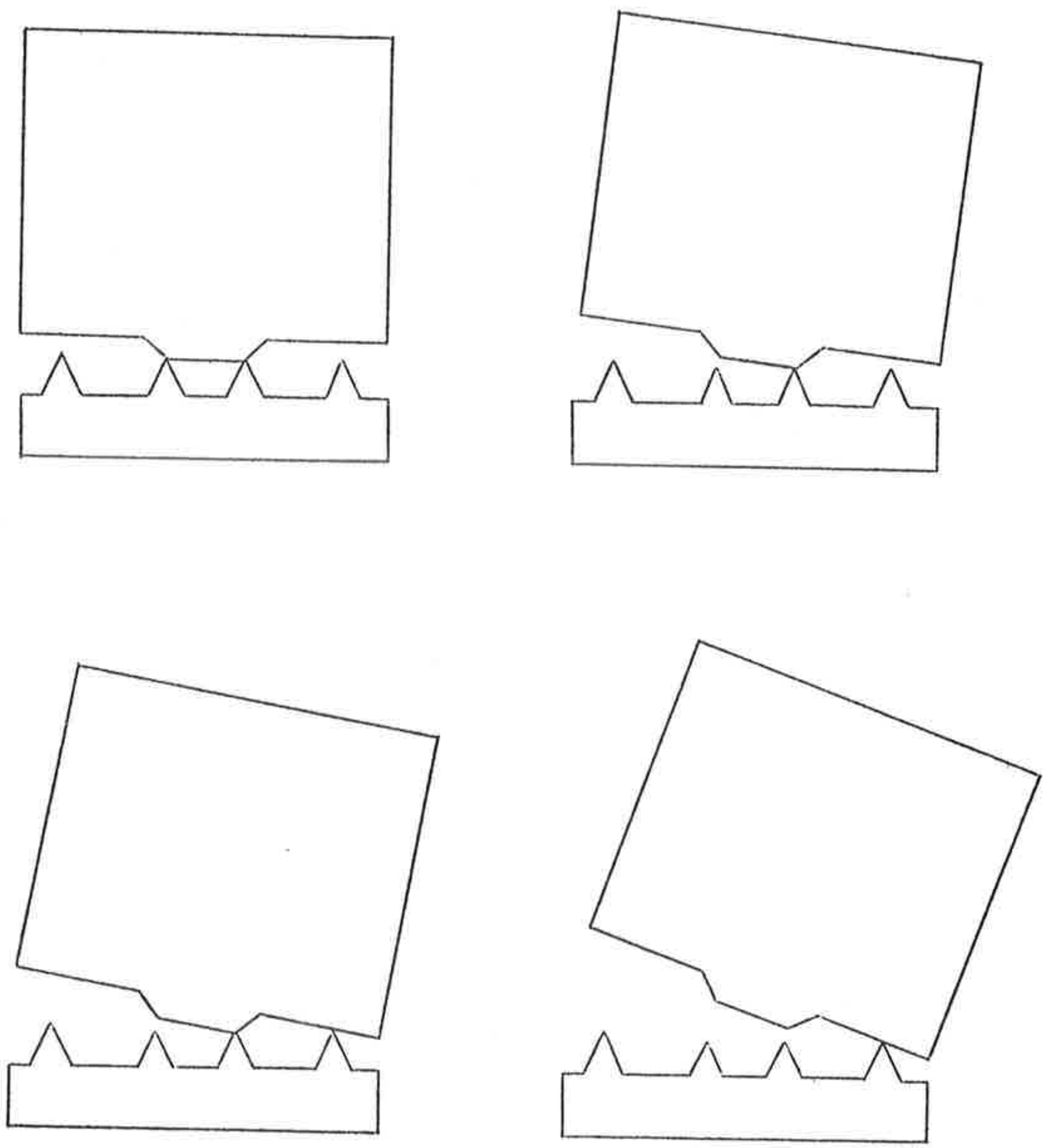

FIGURE 3. FOUR BASIC CAR BODY-BOLSTER RELATIVE POSITIONS CORRESPONDING TO DIFFERENT ROCKING CONDITIONS

body-bolster relative position the contact forces can be computed from the truck model described below.

The truck is represented as a massless framework which is in force and moment equilibrium at each point in time. The front and rear wheelset for the truck are lumped together to yield one equivalent wheelset acting at the truck midpoint and the pitch and yaw motions of the truck are neglected. The vertical displacement of the equivalent single wheelset is computed by adding together the displacement of the front and rear truck right (left) wheels for the right (left) wheel of the equivalent wheelset.

For a truck front to rear wheelset distance B, the track motion can be derived from (1) and (2) as:

$$y_{re} = \frac{A}{2} \left[\left| \sin \frac{\pi V t}{\ell_r} \right| + \left| \sin \frac{\pi (Vt - B)}{\ell_r} \right| \right] , \qquad (6)$$

$$y_{\ell e} = \frac{A}{2} \left[\left| \sin \left(\frac{\pi V t}{\ell_r} + \frac{\pi}{2} \right) \right| + \left| \sin \left(\frac{\pi (Vt - B)}{\ell_r} + \frac{\pi}{2} \right) \right| \right] . \qquad (7)$$

When the wheels are in contact with the track then (6) and (7) define equivalent wheel displacements for the truck left and right sides. When left (right) wheel lift occurs the equivalent wheel left (right) displacement is greater than $y_{\ell e}$ (y_{re}). The computation of wheel lift is discussed below.

In the truck representation, the bolster has vertical, lateral and angular motion while the equivalent wheelset is assumed to have at least one wheel in contact with the track and may rotate about the point of contact or may have both wheels in contact with the track. The suspension group consists of a left and right spring and damper set. Verti-

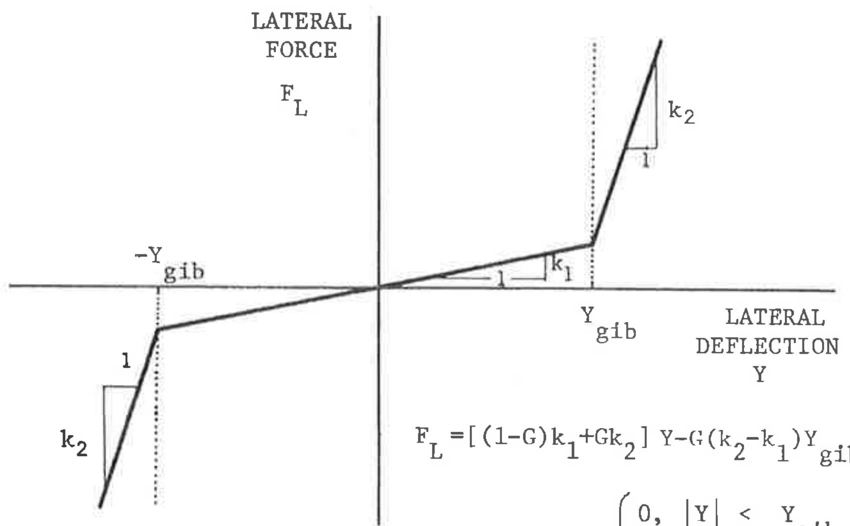

$$F_L = [(1-G)k_1 + Gk_2]\,Y - G(k_2 - k_1)Y_{gib} \cdot sgn[Y]$$

$$G = \begin{cases} 0, & |Y| \leq Y_{gib} \\ 1, & |Y| > Y_{gib} \end{cases}$$

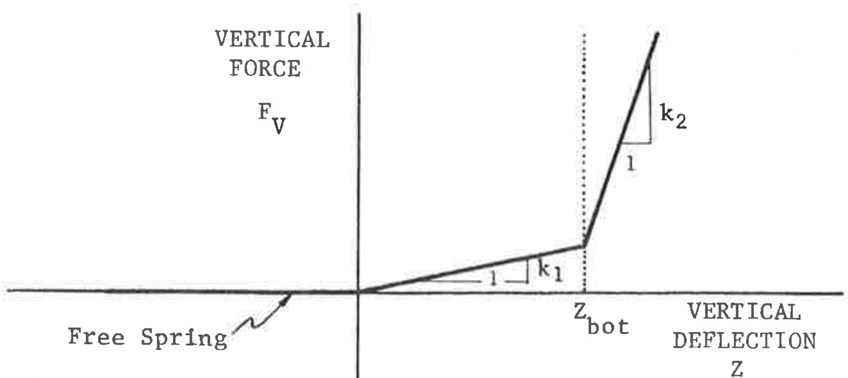

$$F_V = F[(1-B)k_1 + Bk_2]\,Z - B(k_2 - k_1)Z_{bot}$$

$$B = \begin{cases} 0, & Z \leq Z_{bot} \\ 1, & Z > Z_{bot} \end{cases} \quad ; \quad F = \begin{cases} 0, & Z < 0 \\ 1, & Z \geq 0 \end{cases}$$

FIGURE 4 . NONLINEAR LATERAL AND VERTICAL SPRING CHARACTERISTICS REPRESENTING GIB STOPS AND SPRING BOTTOMING

cal springs are modeled as shown in Figure 4 to represent the conditions of a free spring, the spring under normal compression and spring hardening when bottoming occurs. Lateral springs are represented as bilinear with a very steep slope when the lateral displacement exceeds the gib clearance as shown in Figure 4. For both vertical and lateral groups coulomb damping is modeled as a force which is constant with and has its sign determined by the relative velocity between sliding vertical and lateral surfaces.

The truck must be in force and moment equilibrium at each point in time when the inertia effects associated with the wheelsets, the side frames and the bolster are neglected. The force and moment balance equations for the bolster may be expressed in terms of the carbody-bolster contact forces and the left P_L, and right P_R, vertical suspension forces and the lateral suspension force P_H as shown in Figure 5. The force and moment balance equations for the wheelset are summarized in Figure 6. The equations for both the bolster and wheelset depend upon the bolster-car body contact forces, upon the wheel-track forces and the suspension forces P_R, P_L and P_H. These suspension forces are a function of the relative vertical and lateral displacement and velocity across each spring and damper and may be summarized by the constitutive equations

$$P_R = f_1(Z_R) + F_V \cdot \text{sgn}\,[\dot{Z}_R] \tag{8}$$

$$P_L = f_1(Z_L) + F_V \cdot \text{sgn}\,[\dot{Z}_L] \tag{9}$$

$$P_H = f_2(Y_L) + F_H \cdot \text{sgn}\,[\dot{Y}_L] + f_2(Y_R) + F_H \cdot \text{sgn}\,[\dot{Y}_R], \tag{10}$$

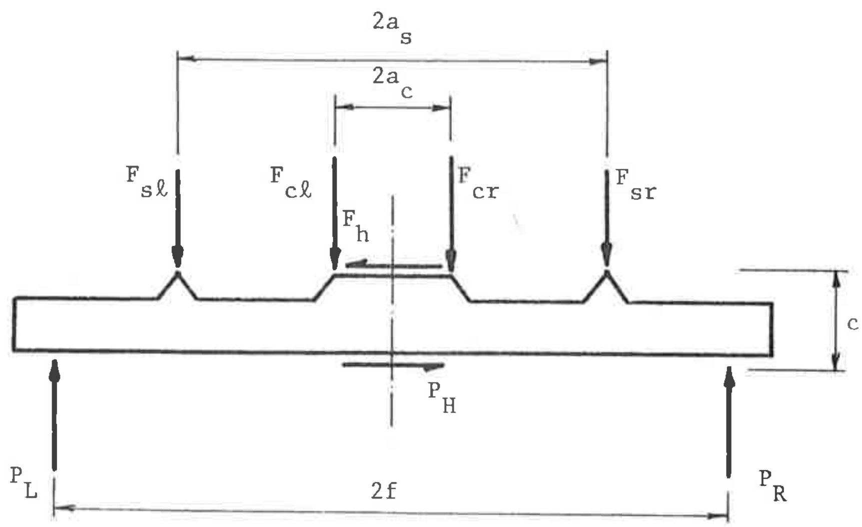

<u>Two Point Contact at Center Plate:</u>

$F_h = P_H,\ F_{sr} = 0,\ F_{s\ell} = 0$

$F_{cr} = [(f+a_c)P_R - (f-a_c)P_L + c \cdot P_H]/2a_c$

$F_{c\ell} = [(f+a_c)P_L - (f-a_c)P_R - c \cdot P_H]/2a_c$

<u>Two Point Contact at Center Plate and Side Bearing-Right:</u>

$F_h = P_H,\ F_{s\ell} = 0,\ F_{c\ell} = 0$

$F_{sr} = [(f-a_c)P_R - (f+a_c)P_L + c \cdot P_H]/(a_s - a_c)$

$F_{cr} = [(f+a_s)P_L - (f-a_s)P_R - c \cdot P_H]/(a_s - a_c)$

<u>One Point Contact at Center Plate-Right:</u>

$F_h = P_H,\ F_{sr} = 0,\ F_{c\ell} = 0,\ F_{s\ell} = 0$

$F_{cr} = P_R + P_L$

<u>One Point Contact at Side Bearing-Right:</u>

$F_h = P_H,\ F_{s\ell} = 0,\ F_{c\ell} = 0,\ F_{cr} = 0$

$F_{sr} = P_R + P_L$

FIGURE 5. FORCES ACTING ON BOLSTER AND COMPUTATION OF CAR BODY/BOLSTER INTERFACE FORCES

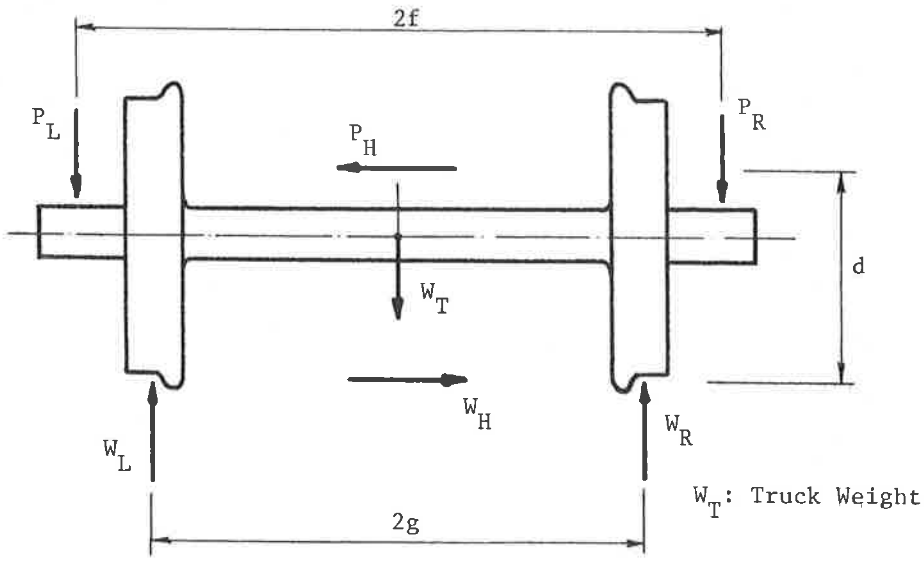

<u>Both Wheels on Rails - No Wheel Lift:</u>

$$W_H = P_H$$

$$W_R = [(f+g)P_R-(f-g)P_L-d\cdot P_H-g\cdot W_T]/2g$$

$$W_L = [(f+g)P_L-(f-g)P_R+d\cdot P_H+g\cdot W_T]/2g$$

<u>Wheel Lift-Right:</u>

$$W_H = P_H$$

$$W_R = 0,\ W_L = P_R + P_L$$

<u>Wheel Lift-Left:</u>

$$W_H = P_H$$

$$W_L = 0,\ W_R = P_R + P_L$$

FIGURE 6. FORCES ACTING ON WHEELSET AND COMPUTATION OF WHEEL/RAIL INTERFACE FORCES

where: $Z_L(Z_R)$ = left (right) suspension group vertical displacement

$Y_L(Y_R)$ = left (right) suspension group lateral displacement

$f_1(Z)$ = vertical spring force - deflection function

$f_2(Y)$ = lateral spring force-deflection function.

F_V = vertical coulomb friction coefficient

F_H = lateral coulomb friction coefficient

The force and moment balance equations summarized in Figures 5 and 6 along with the spring and damper consitutive equations represent a set of algebraic equations which may be solved subject to the kinematic constraints on the truck to yield the suspension forces, the bolster-car body contact forces and wheel-track contact forces. The kinematic constraints are represented by:

a) The geometric constraint that either one or both wheels are in contact with the track.

b) The geometric constraint that the position of the top surface of the bolster is limited by the car body contact points and at any point of contact the bolster velocity matches the car body velocity.

c) The kinematic constraint that in a time period Δt, the relative position X_r is related to the relative velocity $\dot{X}_r$ by

$$X_r = \dot{X}_r \Delta t \ .$$

The search procedure summarized in Figure 7 has been developed to solve the truck bolster and wheelset force and moment balance equations subject to the spring and damper constitutive relations and the constraints cited so that the truck bolster, suspension and wheel forces

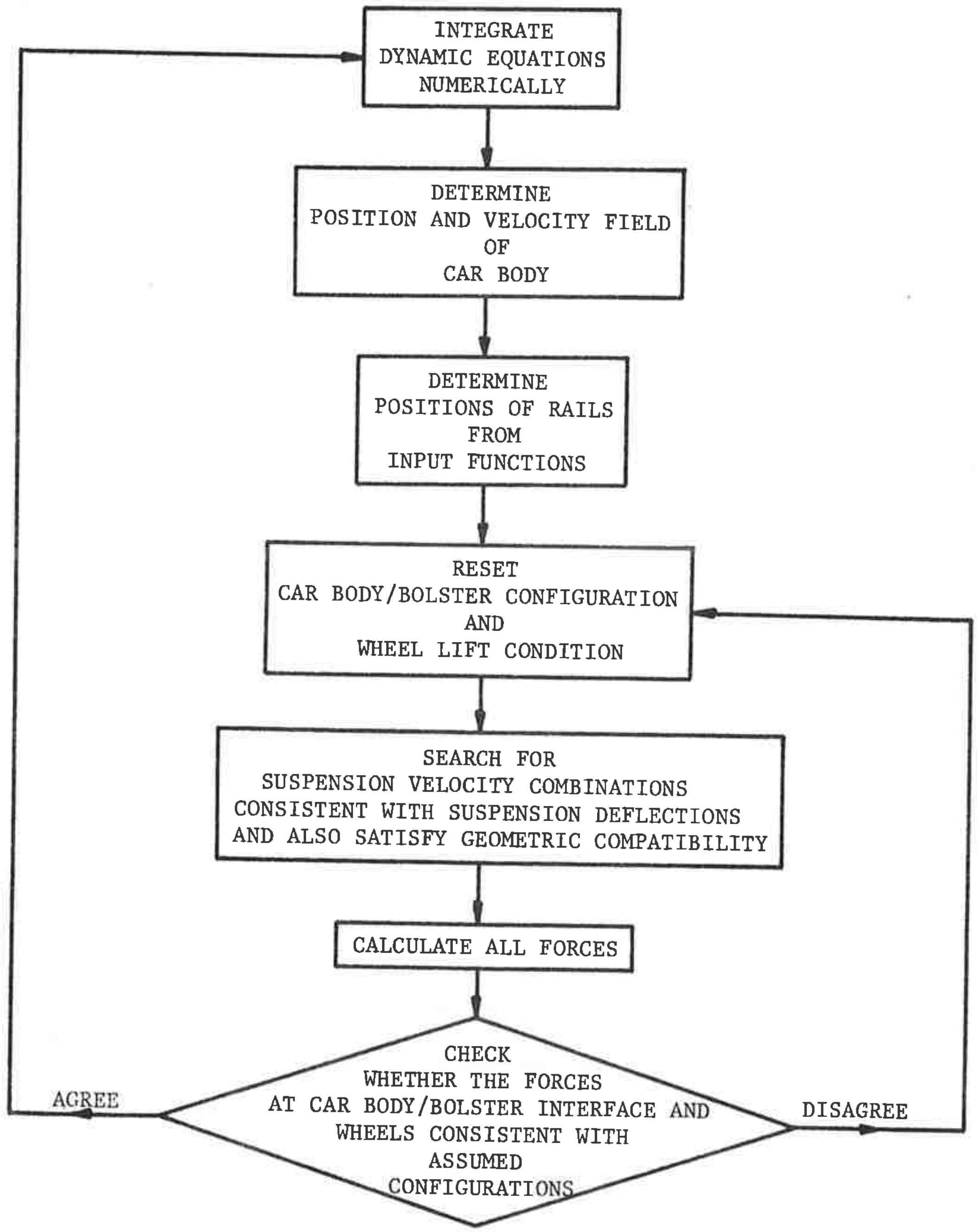

FIGURE 7. SIMULATION COMPUTER PROGRAM FLOW CHART

are determined. Once these forces are determined, they are used in the car body equations to determine the car body accelerations which are integrated to yield velocity and position. Then the car body positions and velocities are used as inputs to the search procedure and the computation repeated for a new point in time.

The model described above has been implemented in a digital computer simulation program for determining the response of both half and full car body model cars. When the full car body model is used yaw and pitch degrees of freedoms are introduced in the car body and an additional set of truck force and moment balance and suspension stiffness and damping equations are introduced.

The computer program has been implemented in Fortran IV language and uses a fourth order Runge-Kutta integration routine, which is similar to that used in the AAR program to integrate the car body equations of motion to determine car body velocity and position.

2.3 Discussion of Model Assumptions in Comparison with More Detailed Simulation Models

The primary difference between the model described above and the more detailed AAR model lies in the neglect of the inertia forces of truck bolster and wheelset. In the AAR model the bolster mass and wheelset mass are included directly. When these mass effects are included, it is necessary also to include track stiffness effects and to model the center plate and side bearing as equivalent stiff springs so that proper computational causality is used. The inclusion of the bolster and wheel set masses acting with these stiff springs introduces high

TABLE 1

APPROXIMATE NATURAL FREQUENCIES ASSOCIATED
WITH DIFFERENT CAR ELEMENTS FOR 70 AND 100 TON FREIGHT CARS

Car Element and Car Type / Frequency and Associated Mode		$\frac{1}{2\pi}\sqrt{\frac{4K_v}{M}}$ Heave	$\frac{1}{2\pi}\sqrt{\frac{4K_h}{M}}$ Sway	$\frac{1}{2\pi}\sqrt{\frac{K_v \ell_s^2}{I + Mh^2}}$ Roll
70 Ton	Car Body	2.17	1.42	0.88
	Wheelset	11.3	7.37	12.5
	Bolster	26.5	17.3	27.7
100 Ton	Car Body	1.88	1.28	0.70
	Wheelset	10.2	6.94	11.7
	Bolster	25.2	17.1	25.0
70 Ton (Unloaded)	Car Body	3.52	2.29	2.18

frequency dynamic motion components into the truck equations. As described in [4-6], these frequencies approach 1000 hertz for the bolster mass acting with the lateral spring stiffness of the gib stop. Because of this high frequency a relatively small, $\Delta t = 0.00025$ sec, integration time interval is required to achieve numerical stability with a fourth order Runge-Kutta integration algorithm.

In the model described in Section 2.2 the bolster and wheelset inertia forces have been neglected. The principal motivation for neglecting these effects is that because of their high frequency content they reach dynamic equilibrium in a time period which is short compared to the car body motion and do not couple dynamically with low frequency car body motion. The approximate frequencies associated with car body motion, bolster and wheelset motions are tabulated in Table 1, computed from simple uncoupled motion for the linear range of spring deflection. The car body heave, sway and roll natural frequencies for the 70 ton and 100 ton fully loaded cars range from 0.7 to 2.17 hertz while for the unloaded 70 ton car the frequencies vary from 2.18 to 3.52 hertz. The frequencies for the bolster and wheelset for the linear range of spring deflections range from 17 to above 20 hertz and are separated by factors of 5-10 from the corresponding car body modes. This wide separation in frequencies results in uncoupling of the dynamic high and low frequency motions. Thus for computation of the primary car body response for input track frequencies which results in severe rocking, i.e., input frequencies of 0-2 hertz, the high frequency bolster and wheelset dynamic motion may be treated quasi-statically and the bolster and wheelset inertial forces neglected.

3. COMPUTATION OF CAR RESPONSE BY DIGITAL SIMULATION

3.1 Response Time Histories

The digital computer simulation program described in Section 2 has been used to determine the responses of 70 and 100 ton freight cars to track cross level variations. The parameters describing the cars are summarized in Table 2. The response of the 70 ton car to a 0.75 in. cross level variation is shown in Figures 8, 9 and 10. In this simulation the car travels at a constant speed of 16.5 mph and at time $t = 0$ encounters the cross level variation. The response illustrates the increase in car rocking response as a function of time to a condition of severe rocking. Plotted in the Figures, as a function of time, are the car body roll angle, the equivalent rail cross level difference input function ($y_{re} - y_{\ell e}$), the car body vertical displacement, the side bearing contact force, wheel lift and wheel force. The Figures show that as the car travels over the irregularities the roll angle increases with each cycle until a maximum roll angle is reached at 12 seconds and then it decreases in the next cycle. The initial roll angle response is in phase with the displacement input, however, as time increases the roll angle lags the input and reaches 180° phase lag by 12 seconds where maximum roll is achieved. The response remains 180° out of phase for time greater than 12 seconds. In this final condition severe rocking occurs with the system and for time periods beyond 12 seconds the response increases again to a maximum value and exhibits a beating pattern. The car body center-of-mass vertical motion illustrates a rapid growth in amplitude and also reaches a maximum in the 12-14 sec.

TABLE 2

PARAMETERS USED IN SIMULATIONS OF 70 AND 100 TON CARS

Car Parameter	70 Ton	100 Ton
Weight of Car Body and Two Bolsters for		
loaded car [lb]...........................	172 650	243 730
empty car [lb]............................	66 000	—
Weight of Each Wheelset [lb]..............	6 380	8 280
Roll Moment of Inertia of Car Body for		
loaded car [lb-in-sec^2]..................	1 288 800	1 824 000
empty car [lb-in-sec^2]...................	346 000	—
Pitch Moment of Inertia of Car Body [lb-in-sec^2]............................	16 650 000	16 800 000
Yaw Moment of Inertia of Car Body [lb-in-sec^2]............................	16 416 000	16 567 000
Suspension Spring Vertical Rate [lb/in]....	20 840	22 110
Suspension Spring Lateral Rate [lb/in].....	8 850	10 200
Gib Stop Lateral Spring Rate at One End of Bolster [lb/in]......................	660 000	55 000
Bottoming Stiffness for Vertical Spring Group [lb/in]............................	660 000	197 100
Vertical Coulomb Friction Force Between Bolster and Side Frame at One End of Bolster [lb]............................	4 000	4 000
Lateral Coulomb Friction Force Between Bolster and Side Frame at One End of Bolster [lb]............................	4 000	4 000
Center Plate Diameter [in]................	14.0	14.0
Height of Car Body CG Above Center Plate		
for Loaded Car...........................	72.5	81.6
Empty Car............................	35.0	—
Height of Center Plate Above Top of the Springs [in]........................	7.875	10.0
Side Bearings Spacing from Center Line [in]..................................	25.0	25.0
Height of Side Bearing Above Top of the Springs [in]........................	12.1875	10.0
Height of Top of the Springs (uncompressed) Above Rails [in]........................	20.125	24.5
Spring Group Spacing from Center Line [in].	39.0	39.52
Half of the Total Gib Clearance [in].......	0.375	0.375
Spring Travel-From Free Height to Bottomed [in]...........................	3.6875	3.6875
Wheel Base [in]...........................	68.0	68.0
Truck Distance [ft].......................	39.0	39.5
Rail Gauge [in]...........................	56.5	56.4
Rail Length [ft]..........................	39.0	39.0

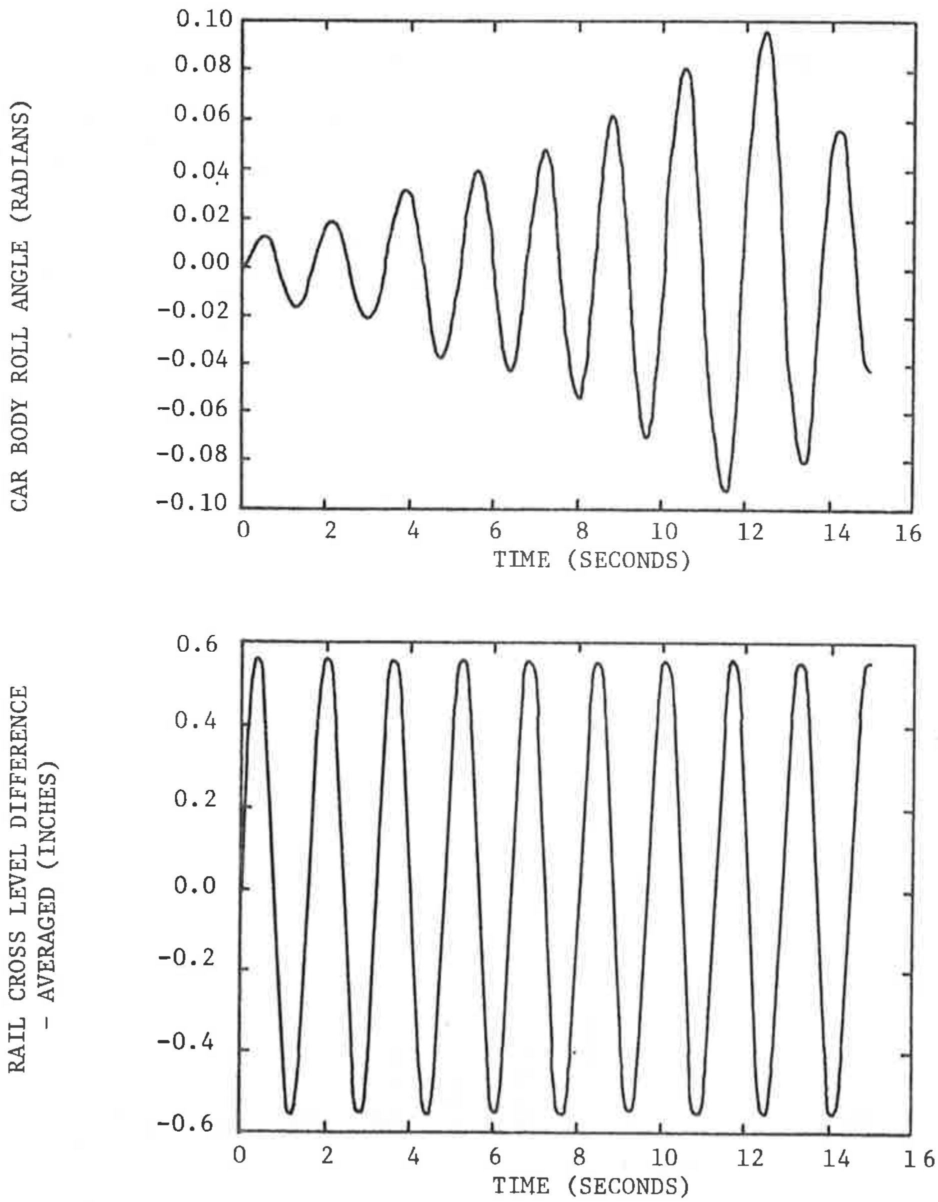

FIGURE 8. TIME HISTORIES OF CAR BODY ROLL ANGLE AND AVERAGED RAIL CROSS LEVEL DIFFERENCE FOR 70-TON CAR WITH 0.75-INCH RAIL CROSS LEVEL DIFFERENCE INPUT AT 16.5 MPH

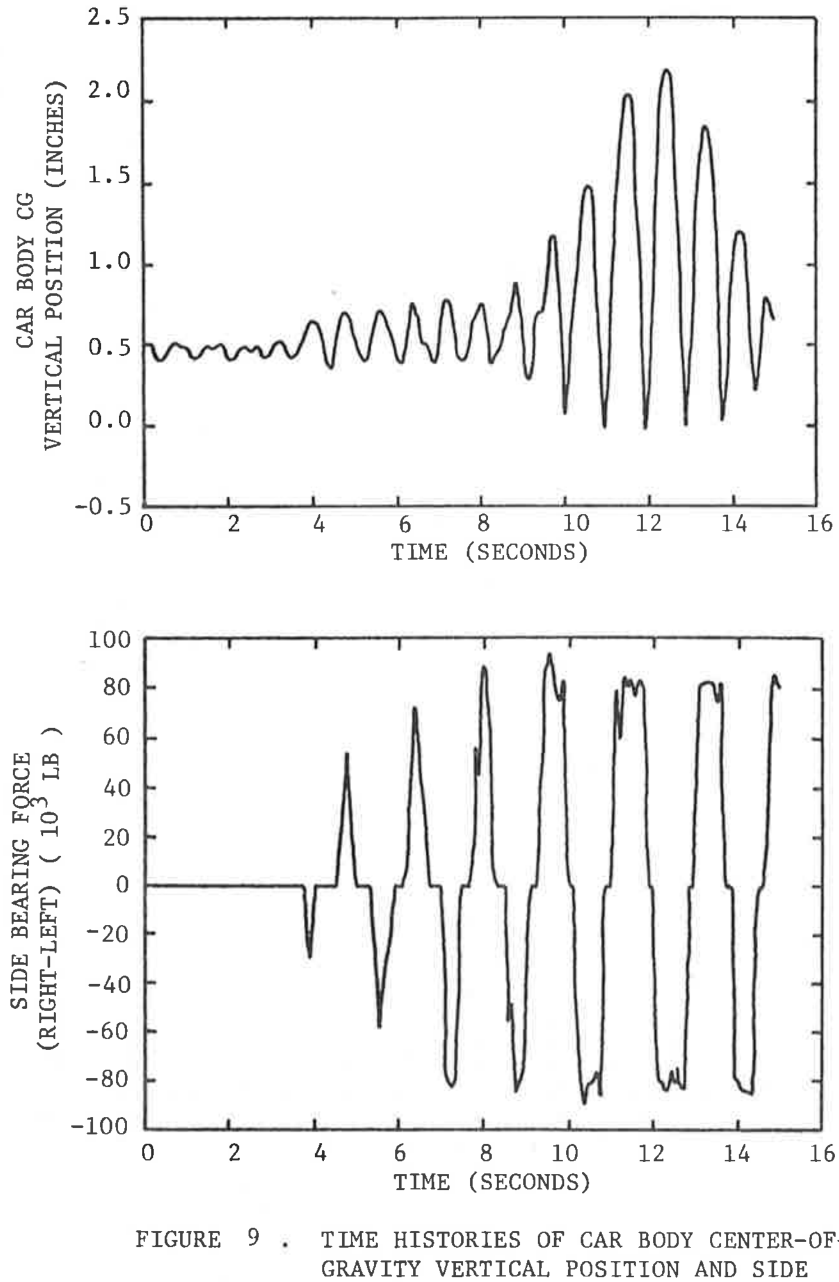

FIGURE 9 . TIME HISTORIES OF CAR BODY CENTER-OF-GRAVITY VERTICAL POSITION AND SIDE BEARING FORCES FOR 70-TON CAR WITH 0.75-INCH RAIL CROSS LEVEL DIFFERENCE INPUT AT 16.5 MPH

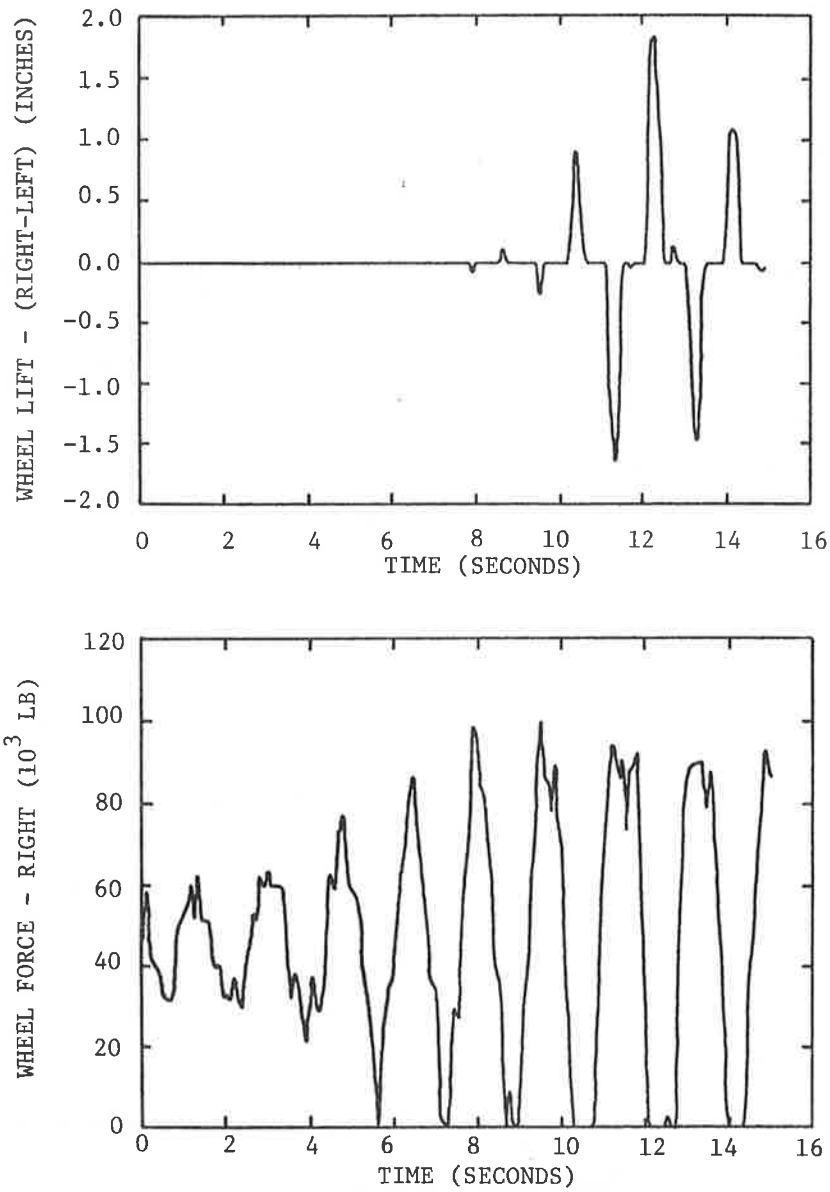

FIGURE 10. TIME HISTORIES OF WHEEL LIFT AND RIGHT WHEEL FORCE FOR 70-TON CAR WITH 0.75-INCH RAIL CROSS LEVEL DIFFERENCE INPUT AT 16.5 MPH

interval. The vertical motion is at double the frequency of the roll motion since for every complete roll cycle, the center of mass raises and lowers twice. While no side bearing contact occurs for the first three "roll cycles" by 4 sec. side bearing contact starts and reaches a maximum value of 90,000 lbs after eight seconds of operation. Wheel lift does not occur for the first eight seconds, however, for the three cycles between 10-14 secs., where severe rocking occurs, significant wheel lift occurs approaching a 2 inch amplitude. The wheel forces also increase significantly under severe rocking so that in the 10-14 second time period, they reach 100,000 lbs which is a factor of almost two times their values for low roll angles in the 0-4 second time period. These time histories illustrate that under large rocking conditions, when wheel lift occurs both side bearing and wheel forces (in the contacting wheel) reach maximum values.

The form of response illustrated in the Figures is typical of time histories computed for the 70 ton car for severe rocking conditions, in which the response grows cycle by cycle, reaches a maximum, then decreases. When the response is compued for longer periods of time, it exhibits a series of "beats" with successive growing and decaying cycles, however, the maximum values achieved in later cycles are similar to those reached in the first series of maximum cycles. Responses computed in an analog computer study [10] have also exhibited this general form and have shown that after 50-100 cycles, the response reaches a nearly steady state pattern. For operating conditions, which do not correspond to severe rocking conditions, the character of the response can change so that the maximum values reached in the first series of cycles are greater than those reached in latter cycles. Because of the strong non-linearities in the freight car response model, it is also possible that for the same set of track and car parameters including operating speeds, several different time responses can be obtained because multiple solutions exist to the non-linear model equations. Which solution is obtained depends upon the car initial conditions as shown in the following section.

3.2 Summary of Car Response Data

Digital simulation runs have been performed for a range of operating speeds for the loaded 70 ton car operating on track with 1.0 inch cross level amplitude. Figure 11 summarizes roll angle response data where the maximum car body roll angle occurring in a simulation time history is plotted for a given speed. As the car speed increases from low speeds below 14 mph light rocking occurs in which the wheel-set, bolster and car body all move together in phase with a car body roll angle of less than 1.5 degrees. As the speed is increased to nearly 14 mph, a sudden jump in roll response occurs as the car body rocks over to contact the side bearings. This region of moderate rocking is charc-terized by a car body roll response which is 90° out of phase with the track cross level amplitude. As the speed is increased further, the response suddenly jumps at 15.5 mph to severe rocking in which center plate separation occurs with significant wheel lift. This region is characterized by a car body response which is 180° out of phase with the track cross level.

The sudden jumps in the response which occur at 14 and 15.5 mph as speed is increased, correspond to changes in the rocking behavior re-

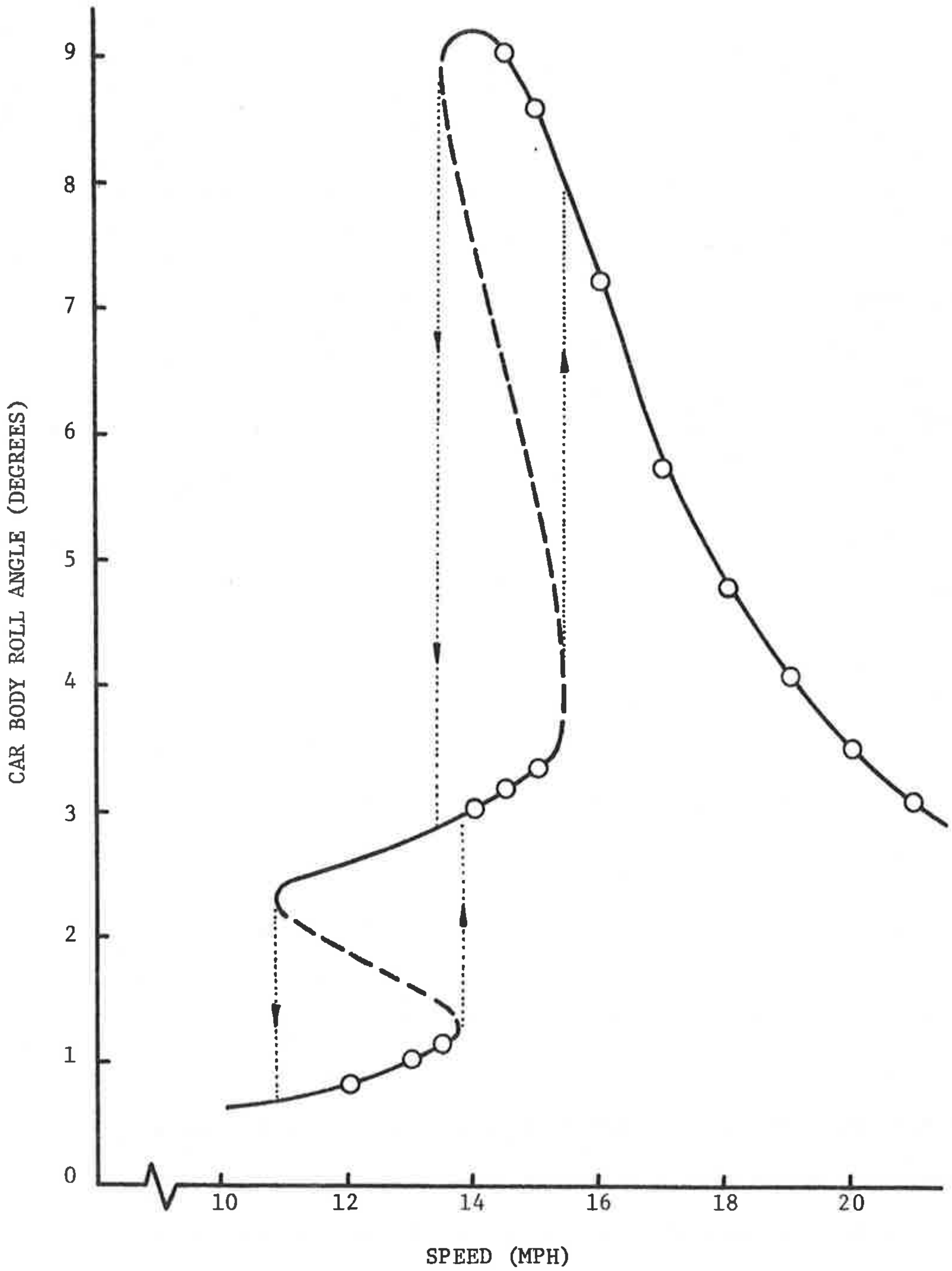

FIGURE 11. CAR BODY ROLL ANGLE FOR 70-TON CAR OBTAINED FROM RESPONSES TO 1-INCH RAIL CROSS LEVEL DIFFERENCE INPUT AT VARIOUS SPEEDS

sulting from a kinematic softening spring effect as the car first rocks off the center plate to touch the side bearings and then leaves the center plate completely. This effect has also been noted qualitatively in [1], [9] and [10] and is common in systems with effective softening springs.

As the speed is increased beyond 15.5 mph, severe rocking persists but at lower amplitude until a car body roll angle of about 3° is reached at 20 mph when moderate rocking occurs. As speed is further increased light rocking occurs again at higher speeds above 25 mph because the track cross level forcing frequency is much greater than the car body resonant frequency.

The car body resonant frequency f_r may be estimated from linear analyses as:

$$f_r = \frac{1}{2\pi}\sqrt{\frac{K_v \ell_s^2}{I+Mh^2}} ,$$

where K_v is the suspension vertical spring rate, ℓ_s the spacing between springs, I is the car body roll moment-of-inertia, M is the car body mass and h is the distance from the track to the car body C.G.. At a speed of $V = f_r \ell_r$ the input frequency matches the car resonant frequency for loaded 70 ton and 100 ton cars, this speed is 20 and 16 mph. For small amplitude disturbances less than 0.5 inch maximum response tends to occur at these speeds. For larger amplitude disturbance such as the 0.75 inch disturbance maximum response occurs at a lower speed of 11-13 mph for the 100 ton car because of the softening spring effect when severe rocking occurs. At speeds high compared with $f_r \ell_r$, the car does not respond to the high frequency input forcing function and rocking angle is decreased.

As speed is decreased from a speed of 20 mph, the roll angle response increases. As speed decreases lower than 15.5 mph, the response continues to increase until 13.5 mph at which speed the response decreases sharply from 9° to 3° as the car changes from severe to moderate rocking. As shown in Figure 11, the maximum amplitude is reached as speed is decreased from 15.5 to 14 mph because of the non-linear softening spring effect. As speed is decreased below 12 mph, the response passes from moderate to light rocking.

The basic jump resonance effect shown in the car model response is a result of the kinematic nonlinearities which occur as center plate side bearing contact is made and finally as complete center plate separation occurs. The amplitude of the response is also influenced by the suspension group vertical and lateral stiffness and damping characteristics, the car body inertia, mass, and length and wheel lift effects. Because of the basic nonlinearities more than one level of roll angle response may be obtained for the car running on a specified track at a given speed. The response level reached depends strongly upon initial conditions, i.e., whether the car enters the condition of interest from a lower or higher speed condition. Thus, different levels of car response may be obtained for nominally the same current conditions, depending upon previous, initial conditions of the car. In Figure 11 the points computed from initial conditions of lower speed are indicated as well as from higher speed by arrows indicating whether the response initial conditions were based upon lower or higher speed operating conditions. Further discussion of response dependence on initial conditions is contained in Section 4.

Data is presented in Figures 12 and 13 showing the amount of wheel lift and center plate, side bearing and wheel forces as a function of speed for the loaded 70 ton car. The wheel lift data shows that no wheel lift occurs for speeds less than 14 mph. The amount of wheel lift is a maximum 2.75 inch at 14.5 mph and as the speed increases, the wheel lift decreases. By 21 mph it has reached 0.5 inch.

The force data show that maximum force levels occur in the 14-16 mph speed range with wheel forces which are 2.3 times the static wheel force.* In this region of operation, forces are generated which are significantly greater than nominal static load forces.

Additional data is presented for the 70 ton car subjected to a 0.75 inch cross level variation in Figure 14 - Roll Angle versus Speed, Figure 15 - Wheel Lift Data versus Speed, and Figure 16 - Force Level Data versus Speed. This data is in general similar to the 1.0 inch data. The maximum roll angle and forces decrease, however. The maximum roll angle at 15 mph decreases from 9° to 7° and the maximum wheel force decreases from 2.3 to 2.1 times the static load.

---

*The force levels cited are for the two wheels on one side of the truck, thus the force for a single wheel is one half the level cited.

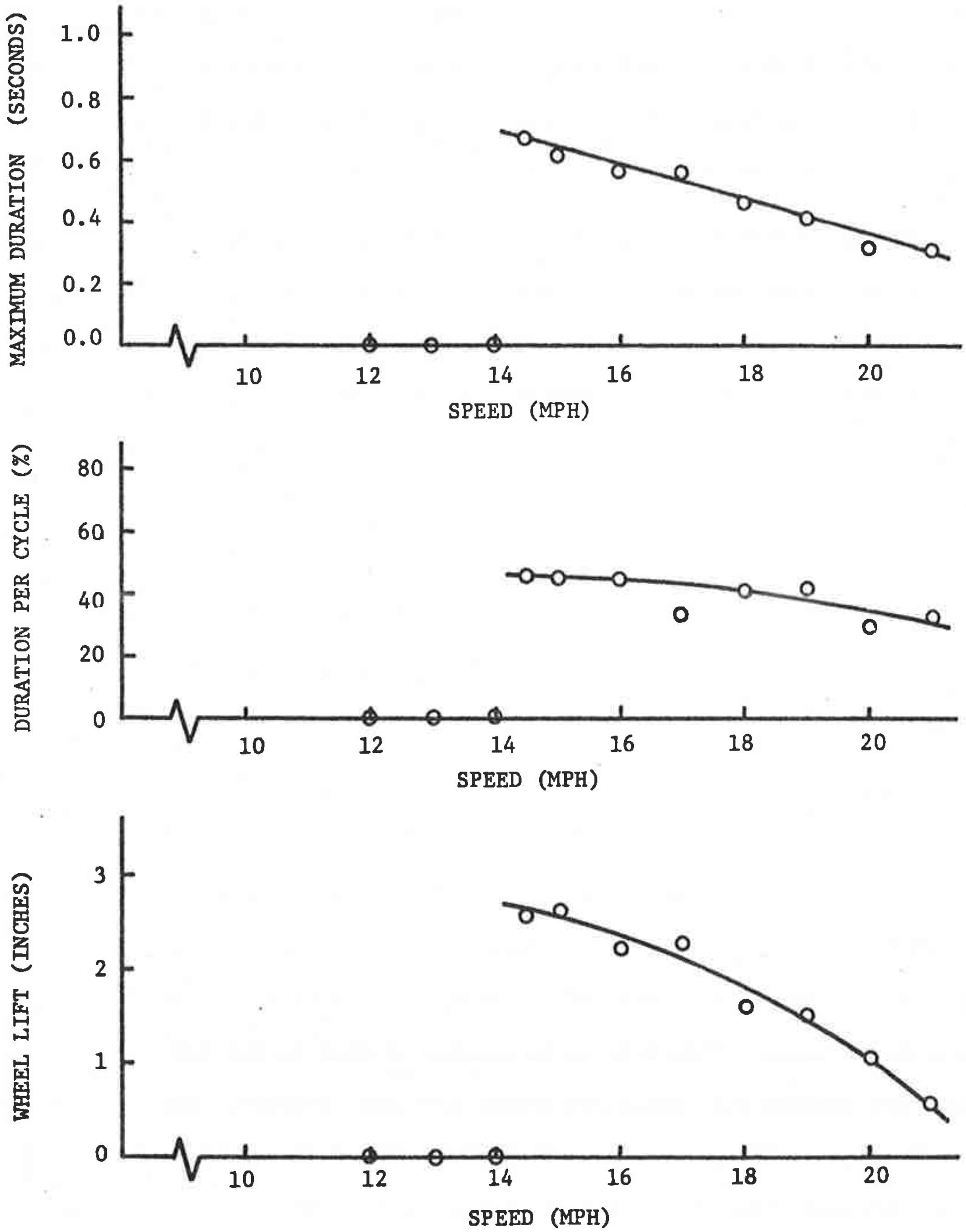

FIGURE 12 . AMOUNT AND DURATION OF WHEEL LIFT FOR 70-TON CAR OBTAINED FROM RESPONSES TO 1-INCH RAIL CROSS LEVEL DIFFERENCE INPUT AT VARIOUS SPEEDS

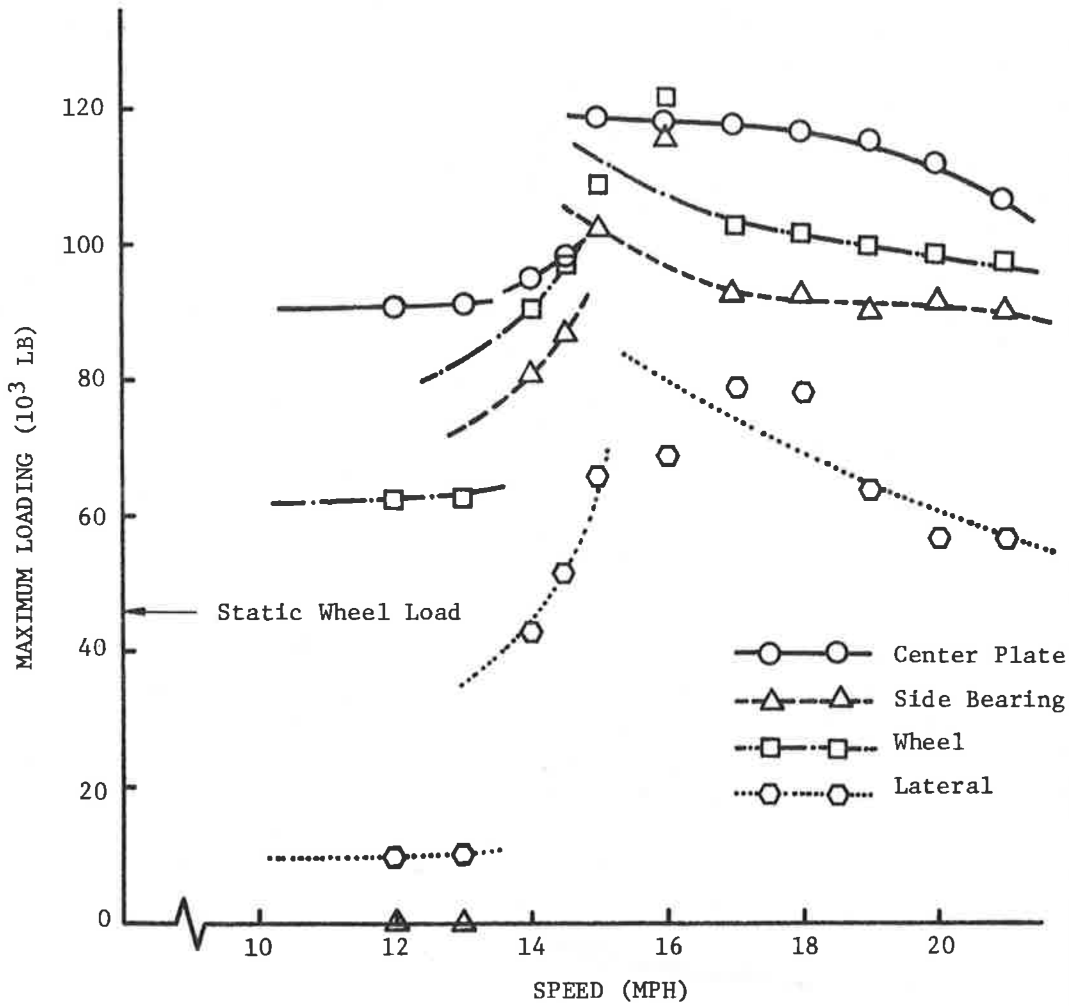

FIGURE 13 . MAXIMUM LOADINGS FOR 70-TON CAR OBTAINED FROM RESPONSES TO 1-INCH RAIL CROSS LEVEL DIFFERENCE INPUT AT VARIOUS SPEEDS

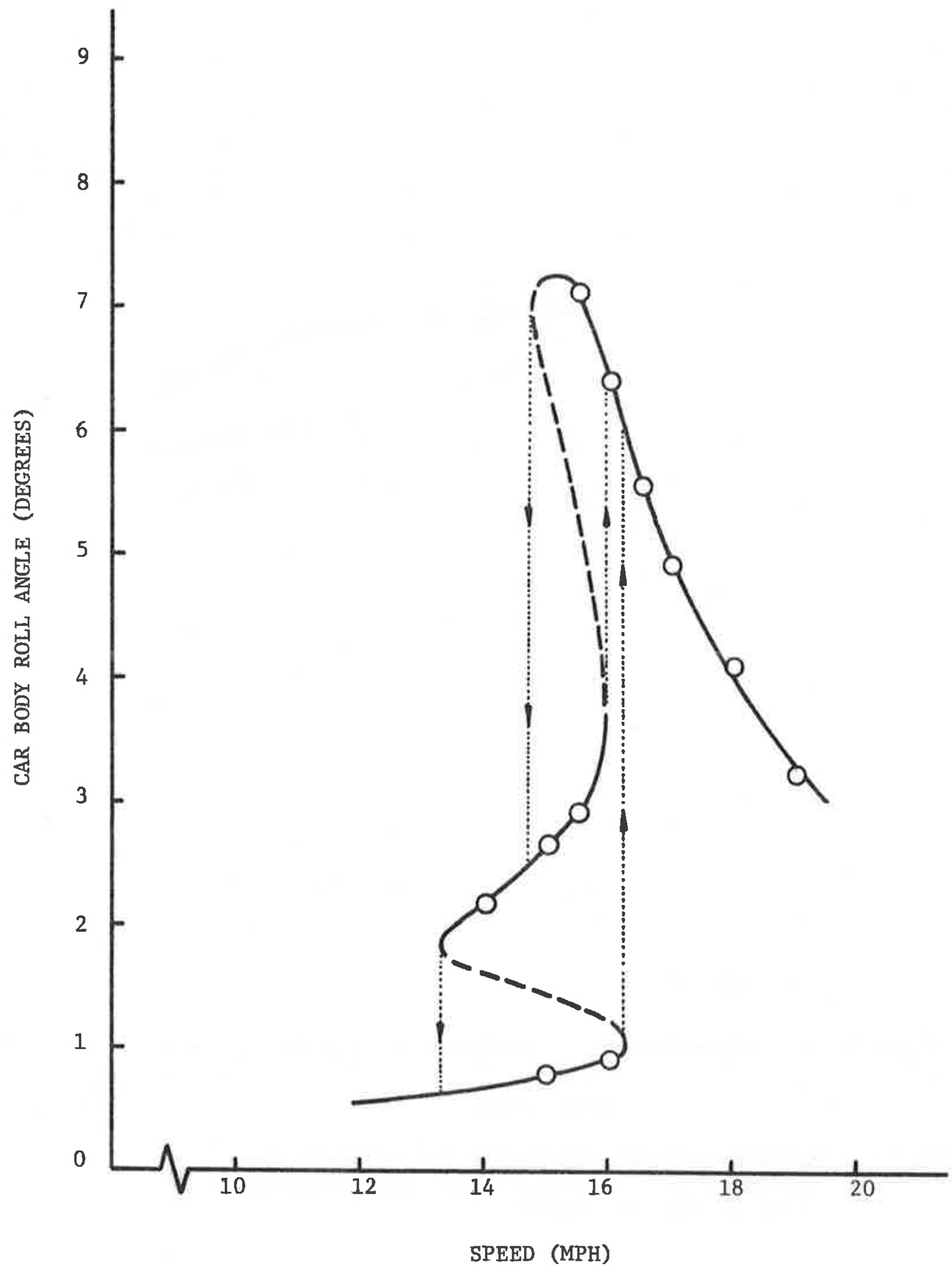

FIGURE 14 . CAR BODY ROLL ANGLE FOR 70-TON CAR OBTAINED FROM RESPONSES TO 0.75-INCH RAIL CROSS LEVEL DIFFERENCE INPUT AT VARIOUS SPEEDS

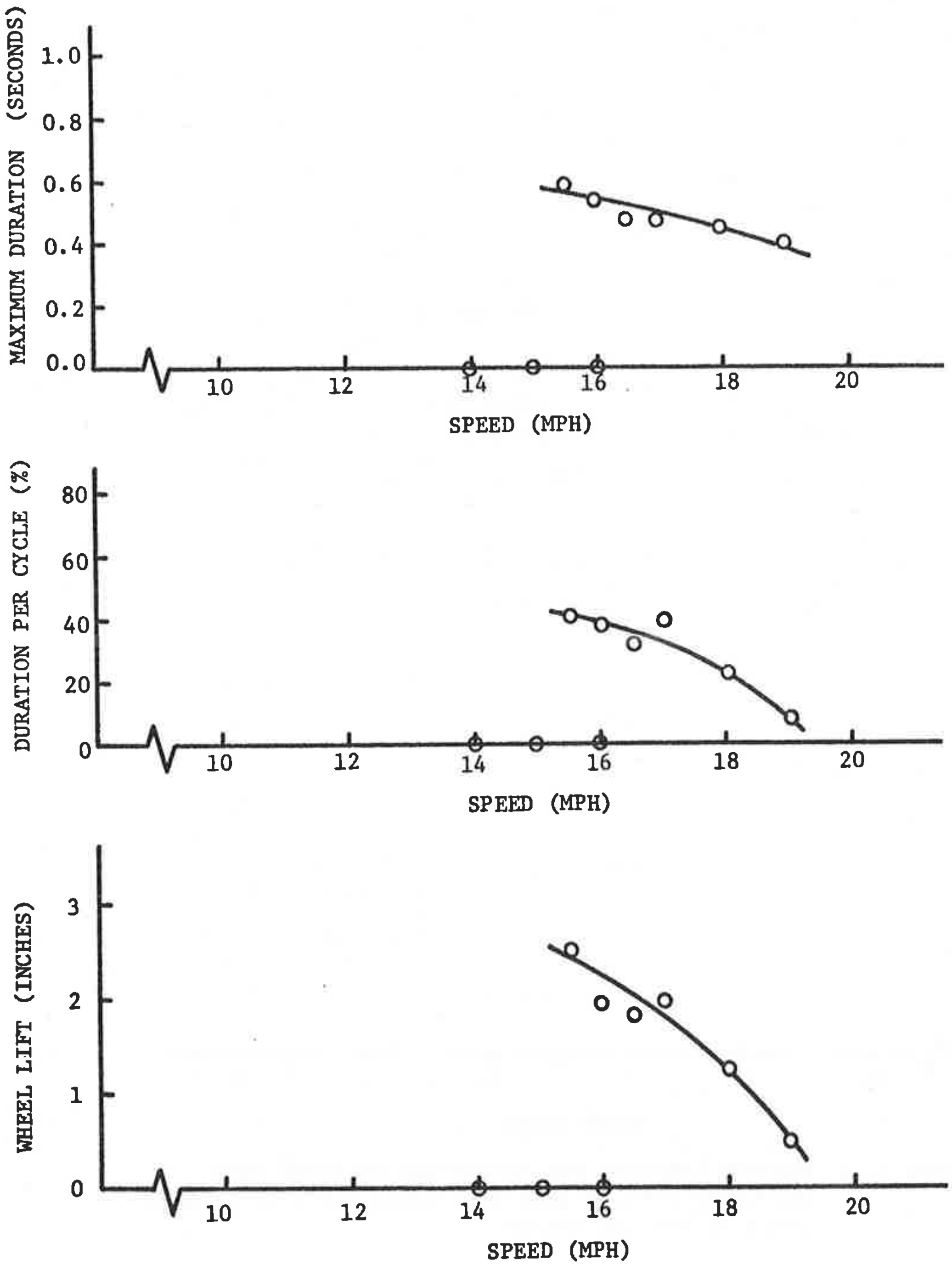

FIGURE 15 . AMOUNT AND DURATION OF WHEEL LIFT FOR 70-TON CAR OBTAINED FROM RESPONSES TO 0.75-INCH RAIL CROSS LEVEL DIFFERENCE INPUT AT VARIOUS SPEEDS

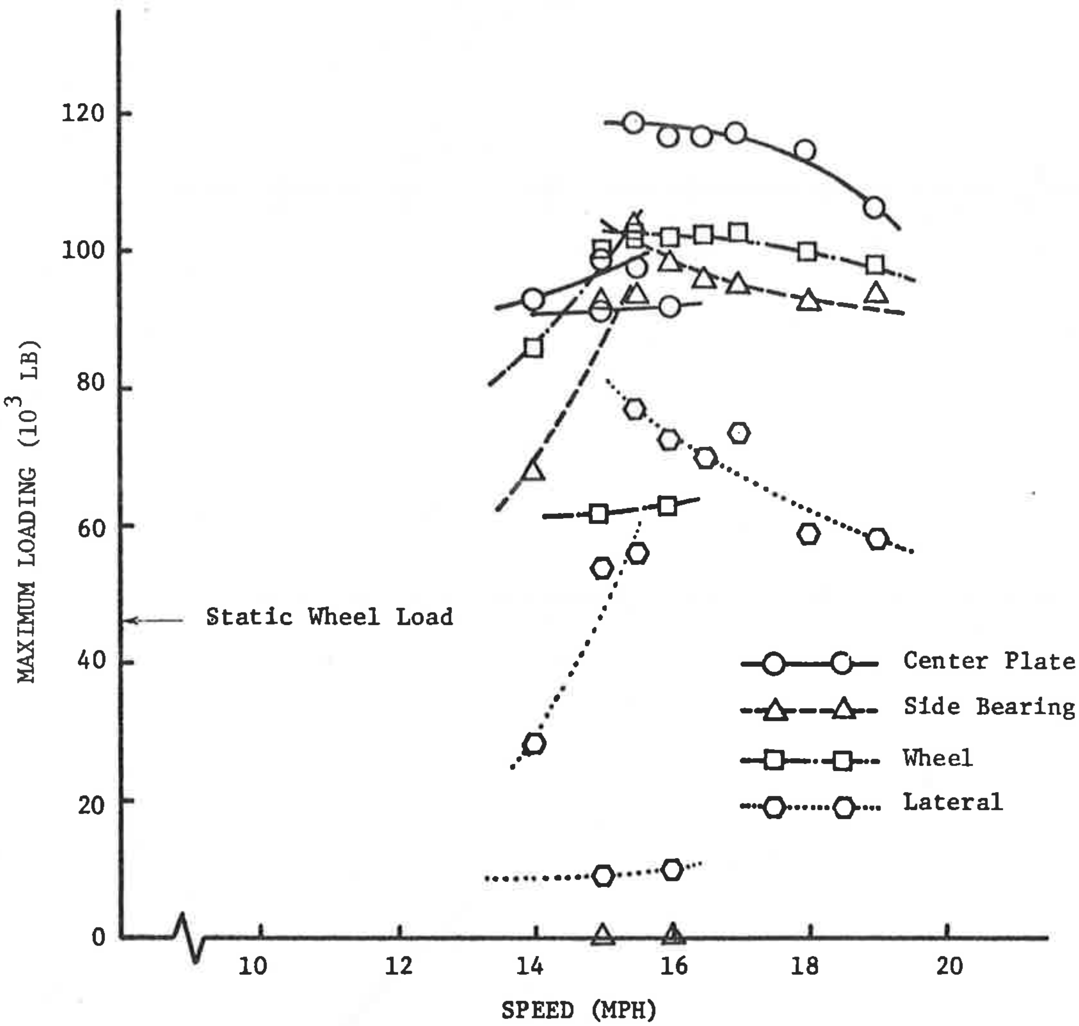

FIGURE 16 : MAXIMUM LOADINGS FOR 70-TON CAR OBTAINED FROM RESPONSES TO 0.75-INCH RAIL CROSS LEVEL DIFFERENCE INPUT AT VARIOUS SPEEDS

Finally, to summarize the influence of cross level variation on the 70 ton car response, roll angle versus speed data has been summarized in Figure 17 for 0.5, 0.75 and 1.0 inch cross level amplitudes. While the data for the 0.75 and 1.0 inch disturbance are similar, the 0.5 inch level disturbance does not generate a heavy rocking response and the maximum rocking response is less than 1.5°.*

Data for a 70 ton empty car response to 0.75 inch track cross level variations is presented in Figures 18, 19 and 20. For the empty car, the maximum response occurs at 30 mph. The maximum roll angle is less than 3.5° and maximum wheel loads are less than 60,000 lbs. Thus, the empty car has a maximum response speed which is nearly twice that of the full car and maximum wheel loads and roll angles which are less than 60% of those of a full car.

Complete sets of response data to 0.75 and 1.0 inch cross level disturbances for a full 100 ton car with the properties cited in Table 2 are summarized in Figure 21-26. Response data for the 100 ton car are similar in form to those for the 70 ton with the maximum response occuring at 13 mph. The roll angle response versus speed illustrates a jump resonance at 13 mph for which the maximum roll angle reaches 6.8° for 0.75 inch and 8° for the 1.0 inch cross level amplitude inputs. The maximum wheel forces in the 100 ton car for the 1.0 inch cross level amplitude occur at 13 mph and reach approximately three times the static wheel forces. Dynamic wheel

---

* Note discussion in Section 4 in which it is shown that while difficult to achieve, theoretically a heavy rocking response exists for this case.

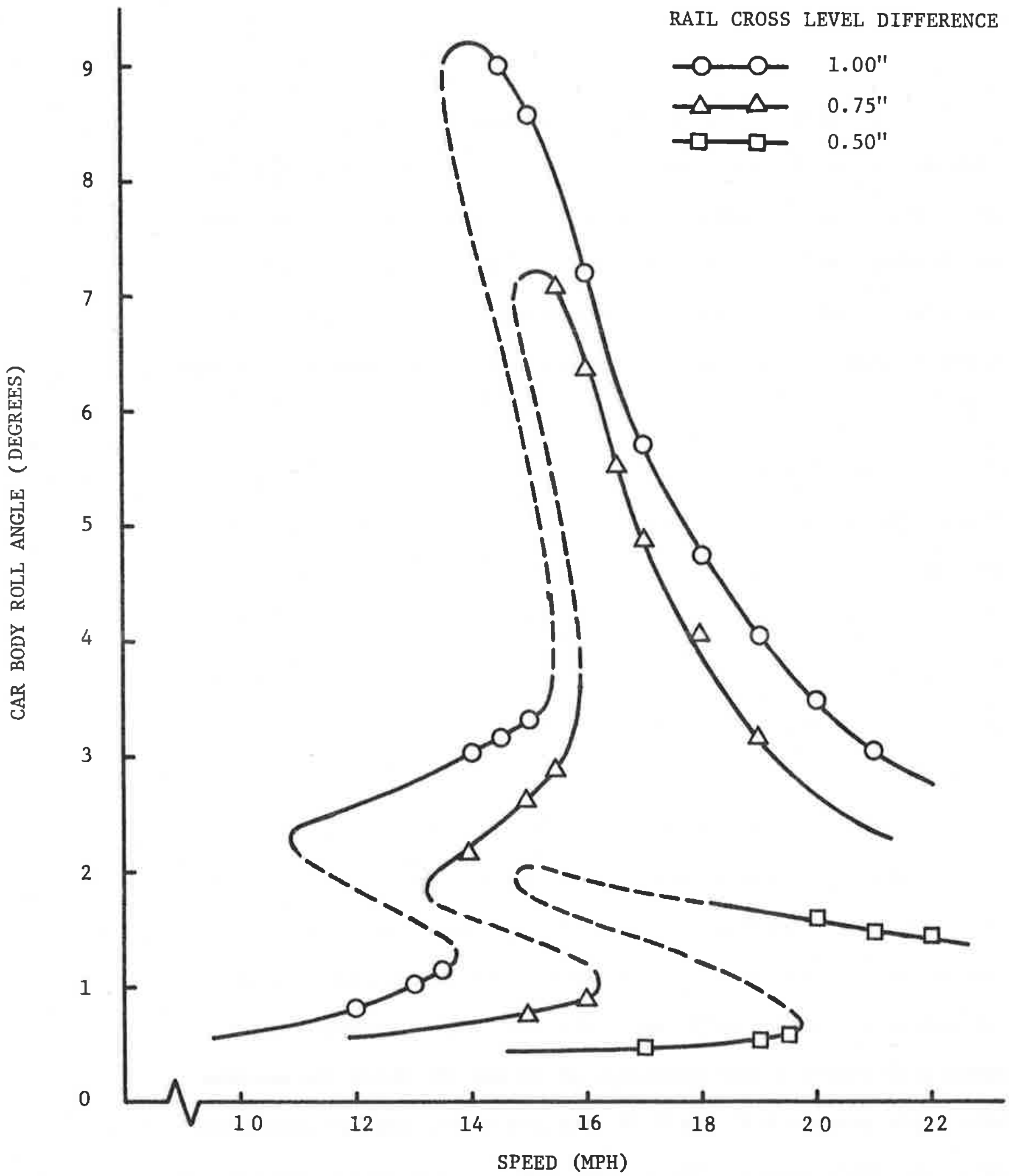

FIGURE 17. COMPARISON OF CAR BODY ROLL ANGLE RESPONSES TO DIFFERENT RAIL CROSS LEVEL DIFFERENCE INPUTS FOR 70-TON CAR

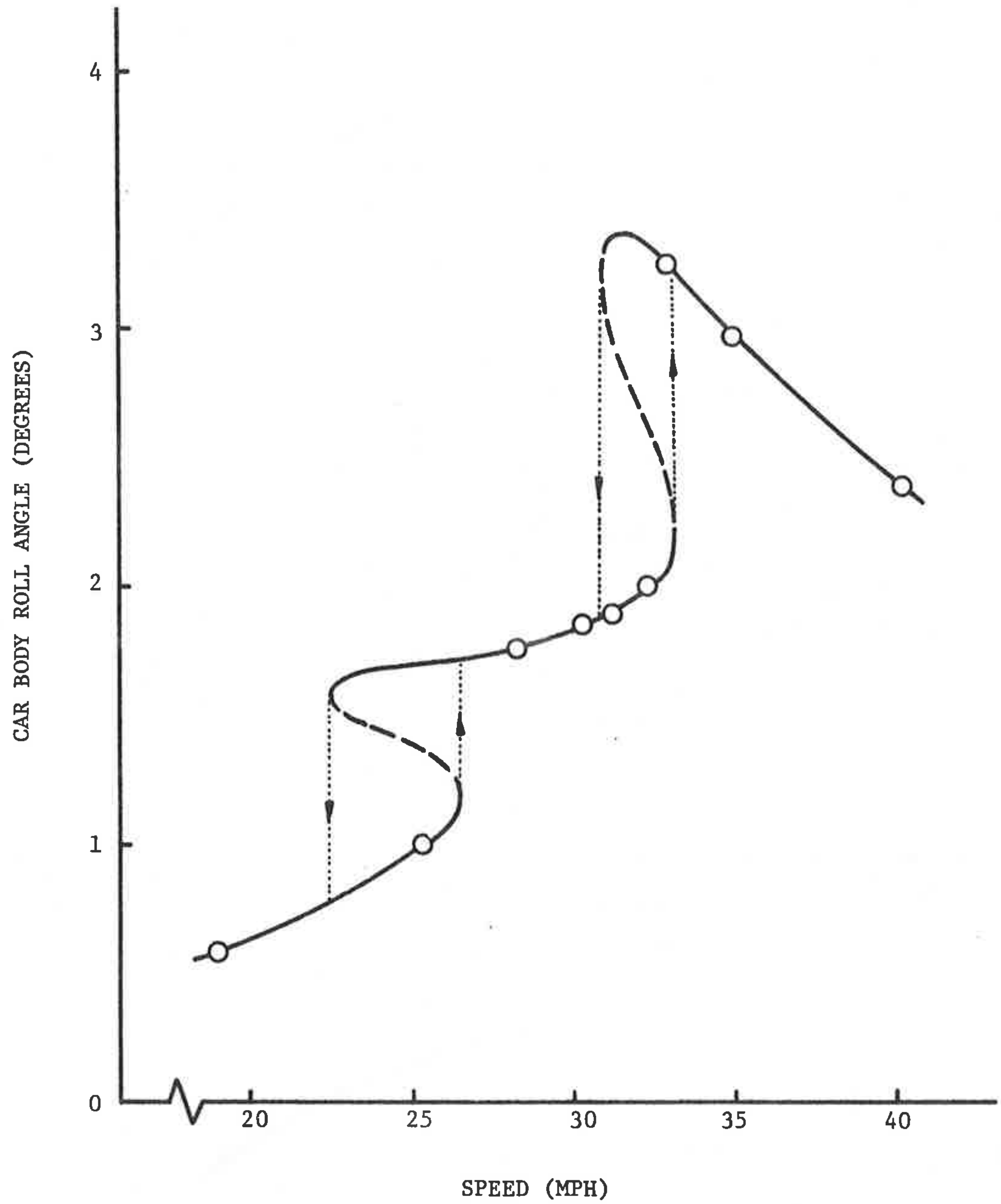

FIGURE 18 . CAR BODY ROLL ANGLE FOR 70-TON EMPTY CAR OBTAINED FROM RESPONSES TO 0.75-INCH RAIL CROSS LEVEL DIFFERENCE INPUT AT VARIOUS SPEEDS

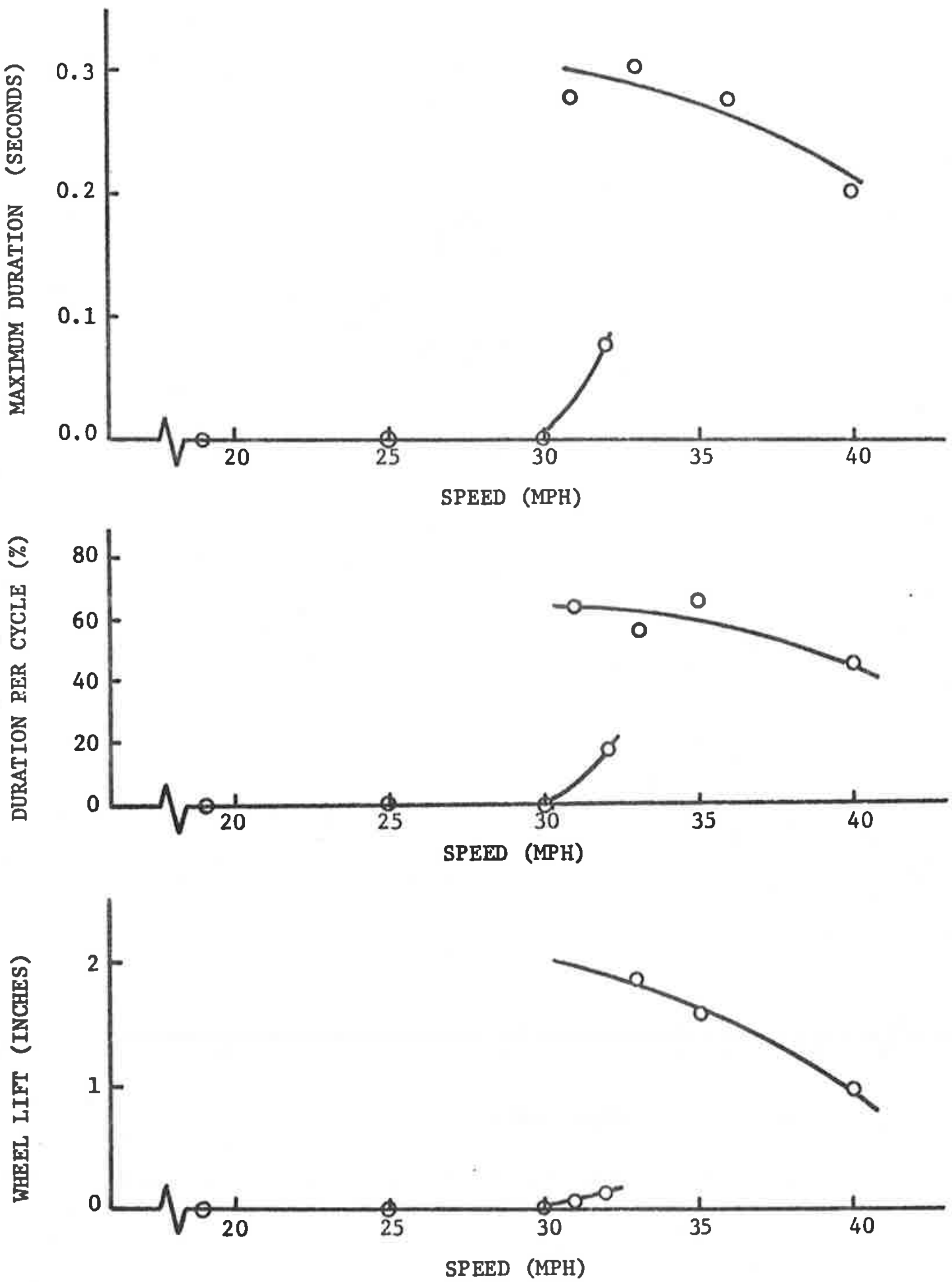

FIGURE 19 . AMOUNT AND DURATION OF WHEEL LIFT FOR 70-TON EMPTY CAR OBTAINED FROM RESPONSES TO 0.75-INCH RAIL CROSS LEVEL DIFFERENCE AT VARIOUS SPEEDS

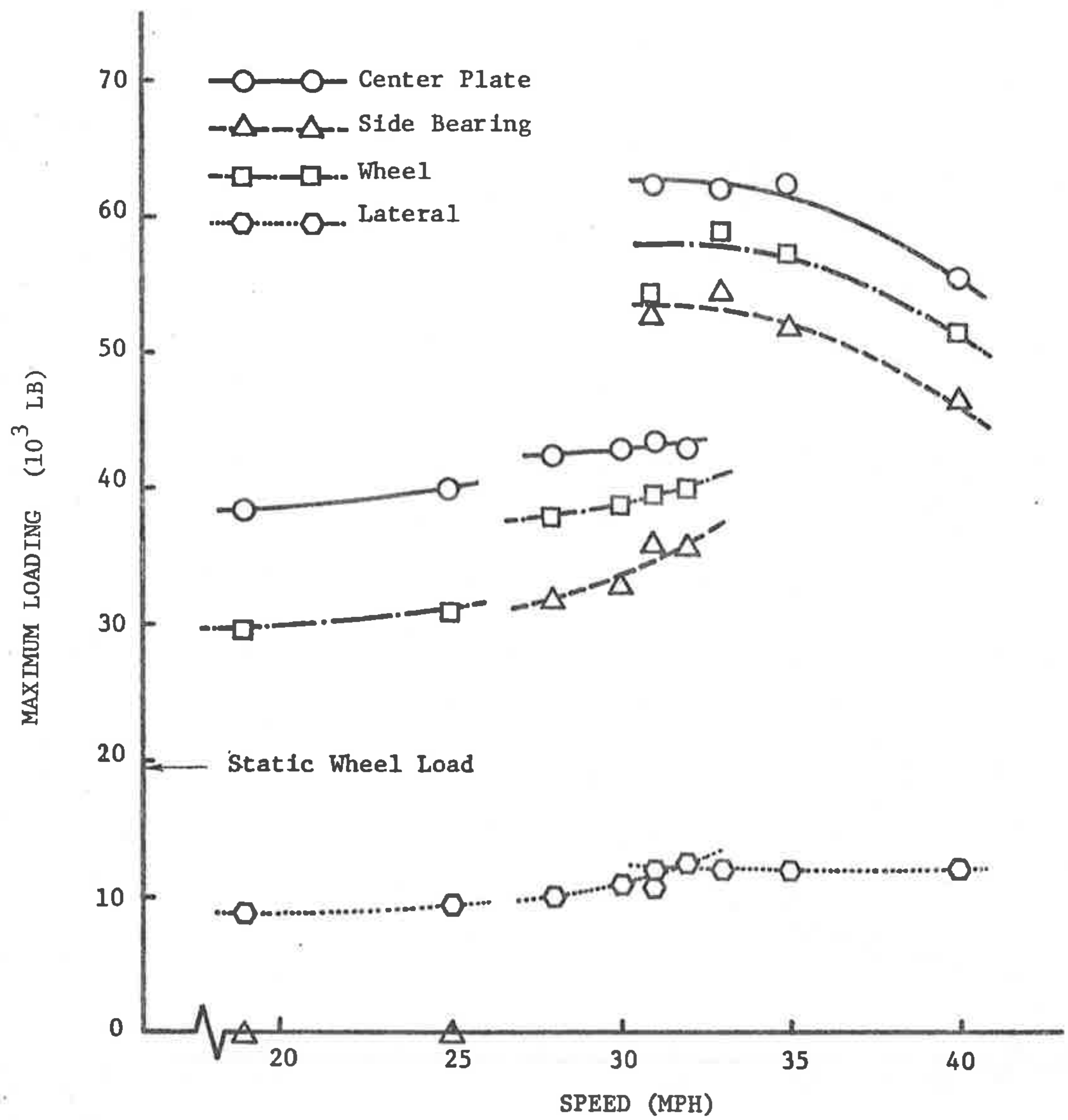

FIGURE 20 . MAXIMUM LOADINGS FOR 70-TON EMPTY CAR OBTAINED FROM RESPONSES TO 0.75-INCH RAIL CROSS LEVEL DIFFERENCE INPUT AT VARIOUS SPEEDS

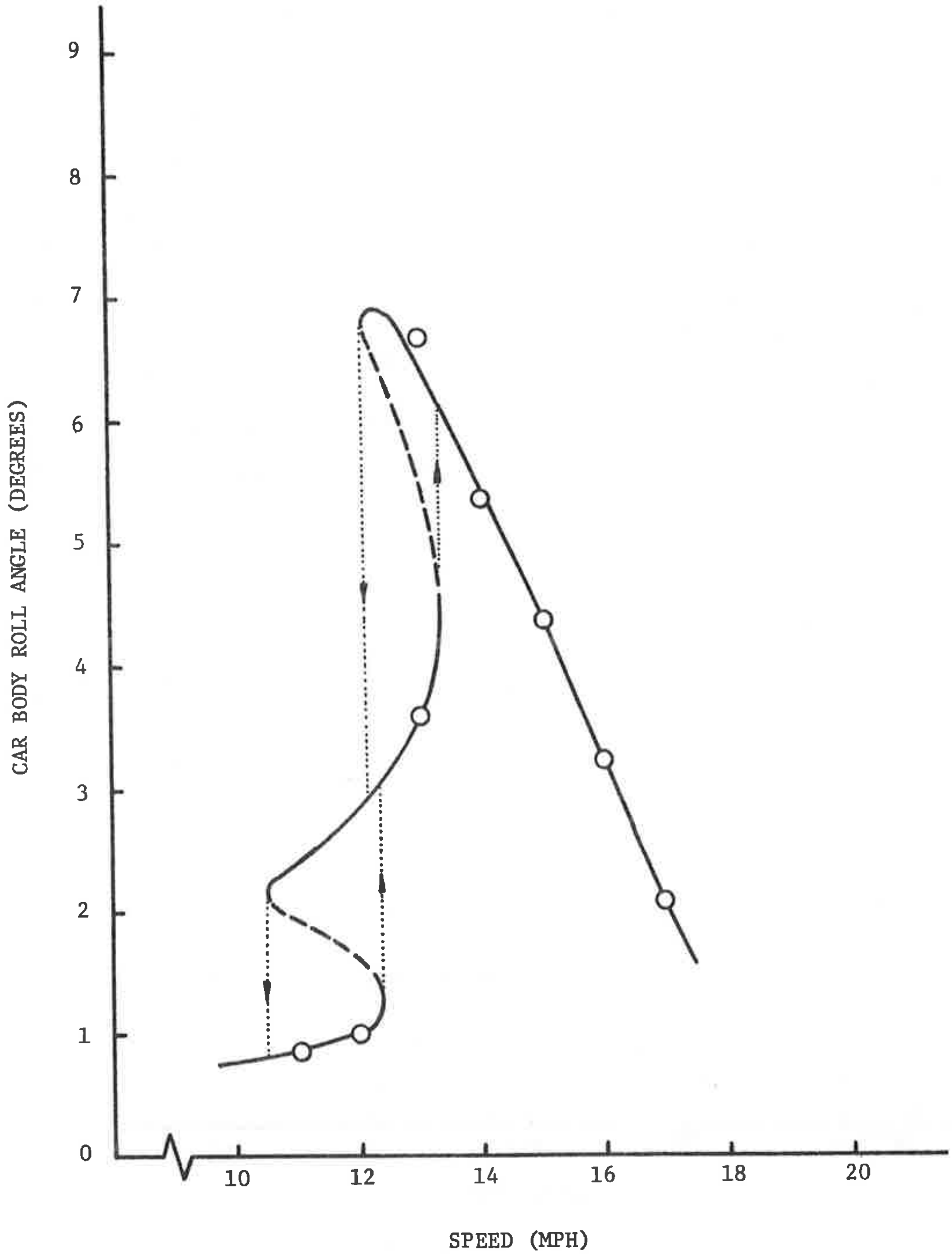

FIGURE 21. CAR BODY ROLL ANGLE FOR 100-TON CAR OBTAINED FROM RESPONSES TO 0.75-INCH RAIL CROSS LEVEL DIFFERENCE INPUT AT VARIOUS SPEEDS

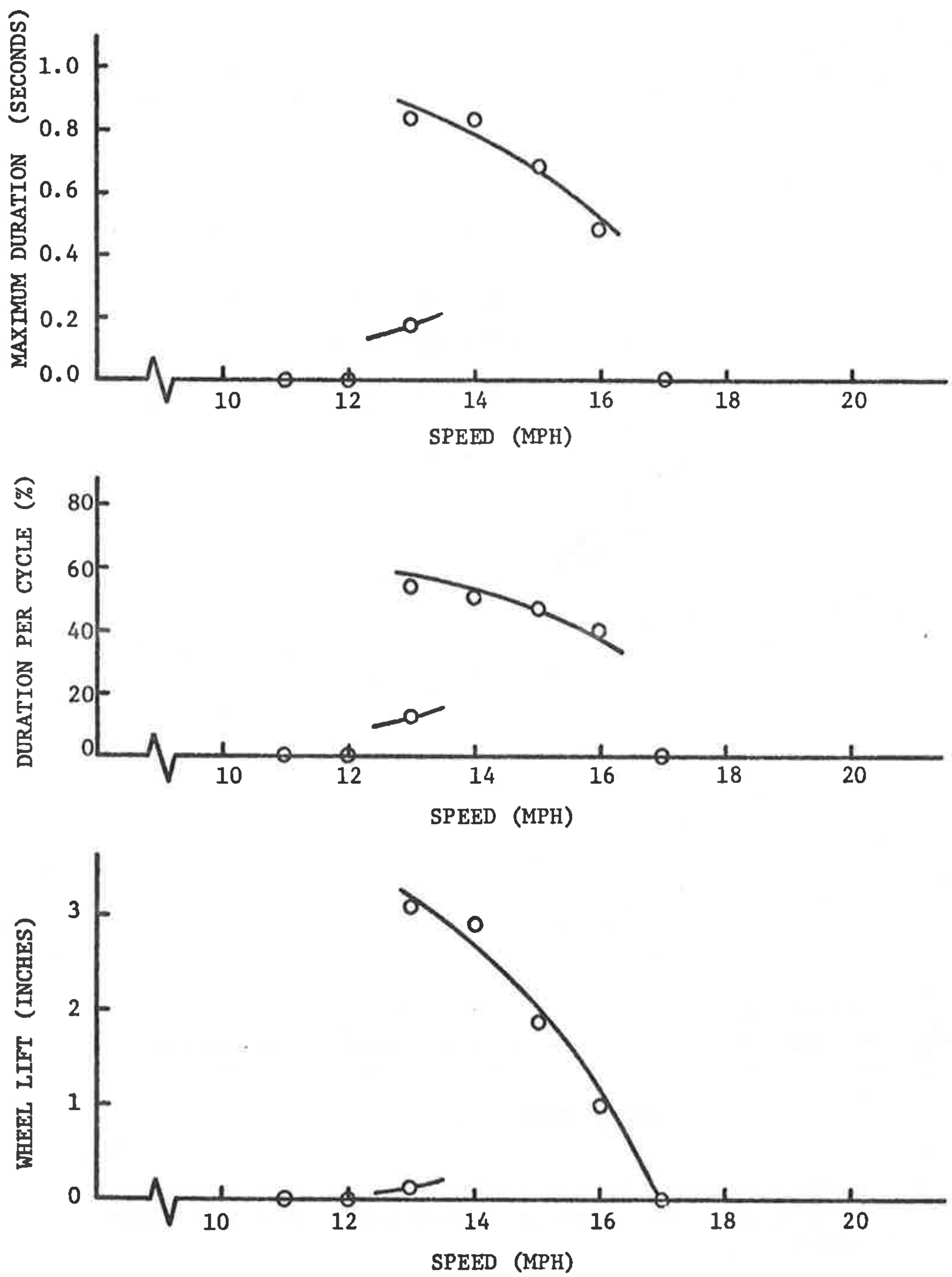

FIGURE 22 . AMOUNT AND DURATION OF WHEEL LIFT FOR 100-TON CAR OBTAINED FROM RESPONSES TO 0.75-INCH RAIL CROSS LEVEL DIFFERENCE AT VARIOUS SPEEDS

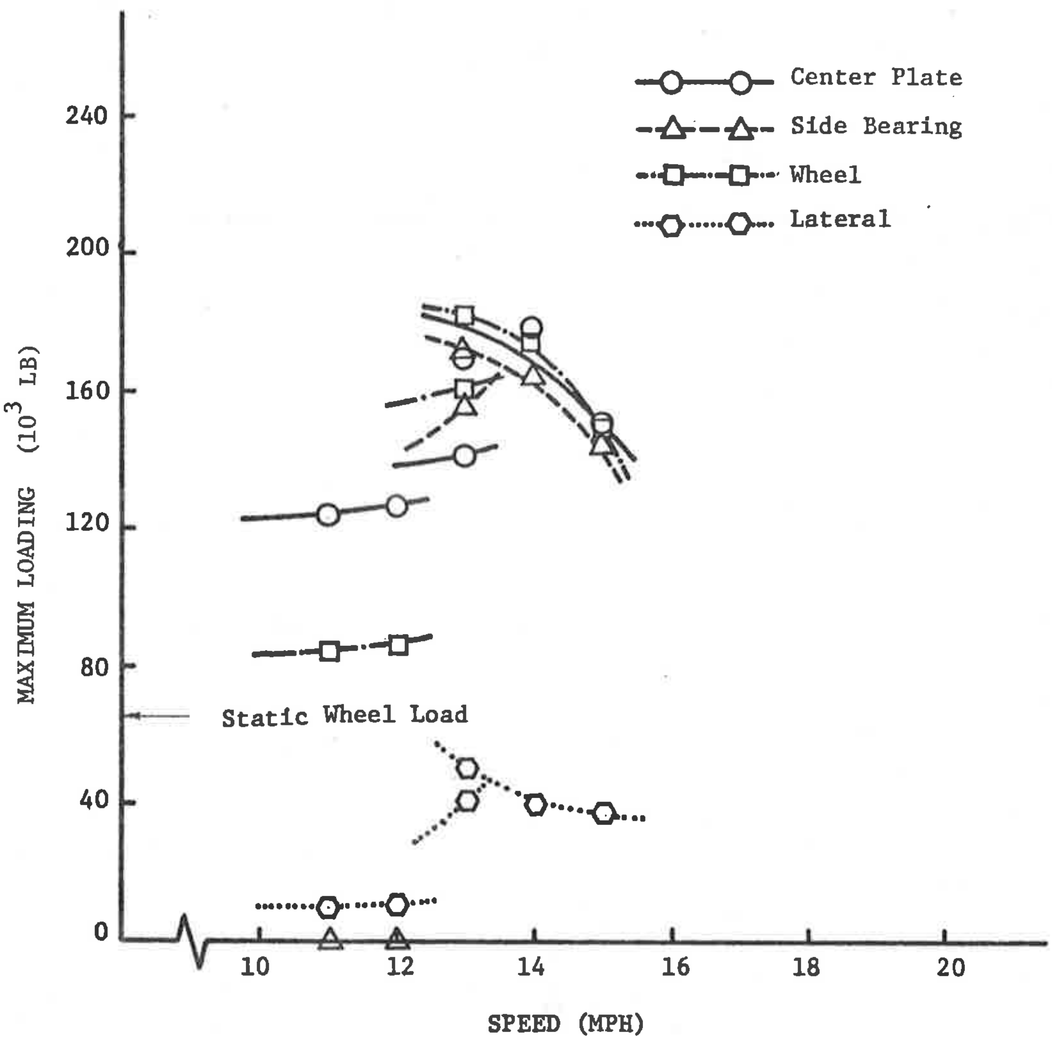

FIGURE 23 . MAXIMUM LOADINGS FOR 100-TON CAR OBTAINED FROM RESPONSES TO 0.75-INCH RAIL CROSS LEVEL DIFFERENCE INPUT AT VARIOUS SPEEDS

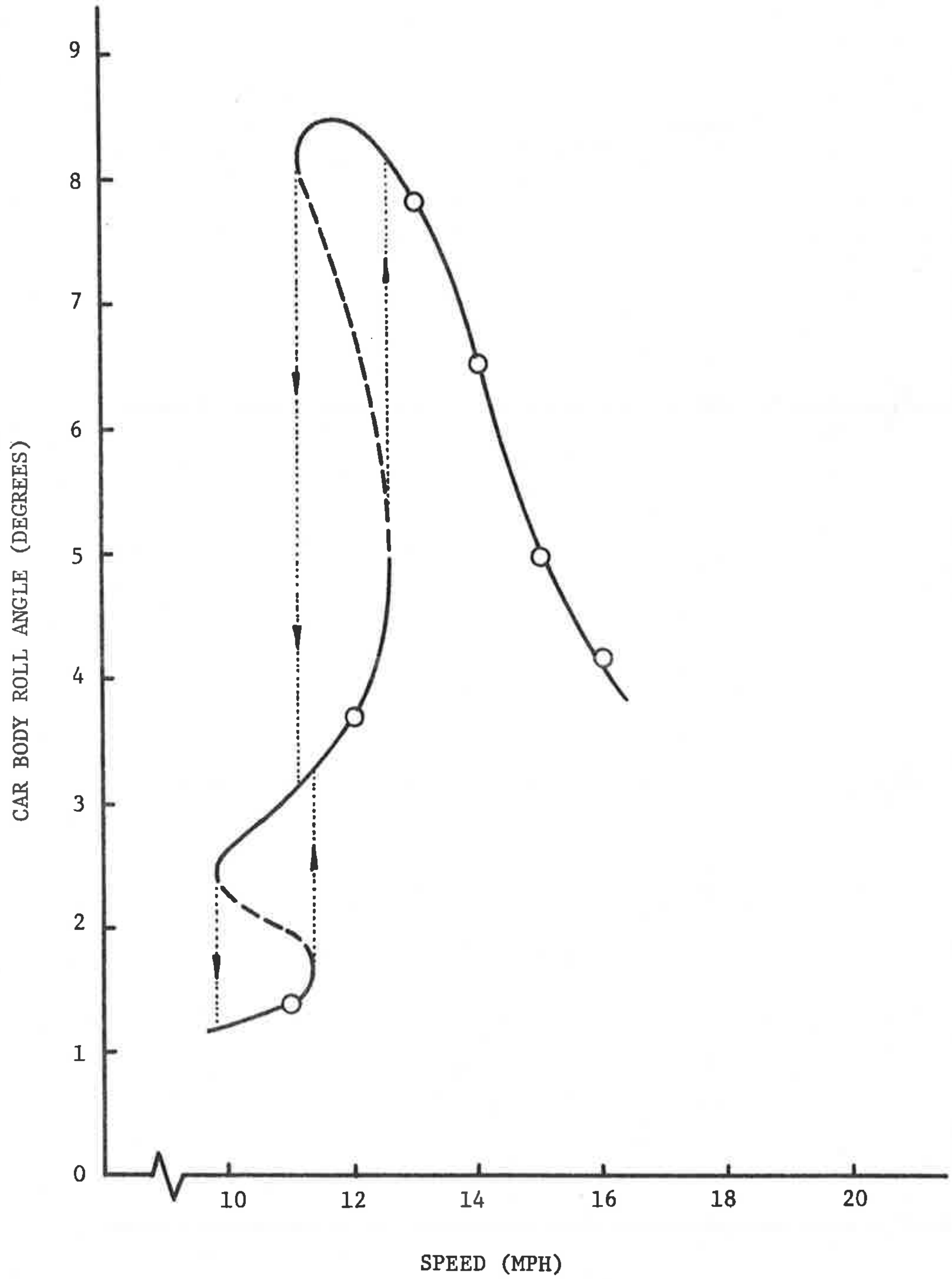

FIGURE 24 . CAR BODY ROLL ANGLE FOR 100-TON CAR OBTAINED FROM RESPONSES TO 1-INCH RAIL CROSS LEVEL DIFFERENCE INPUT AT VARIOUS SPEEDS

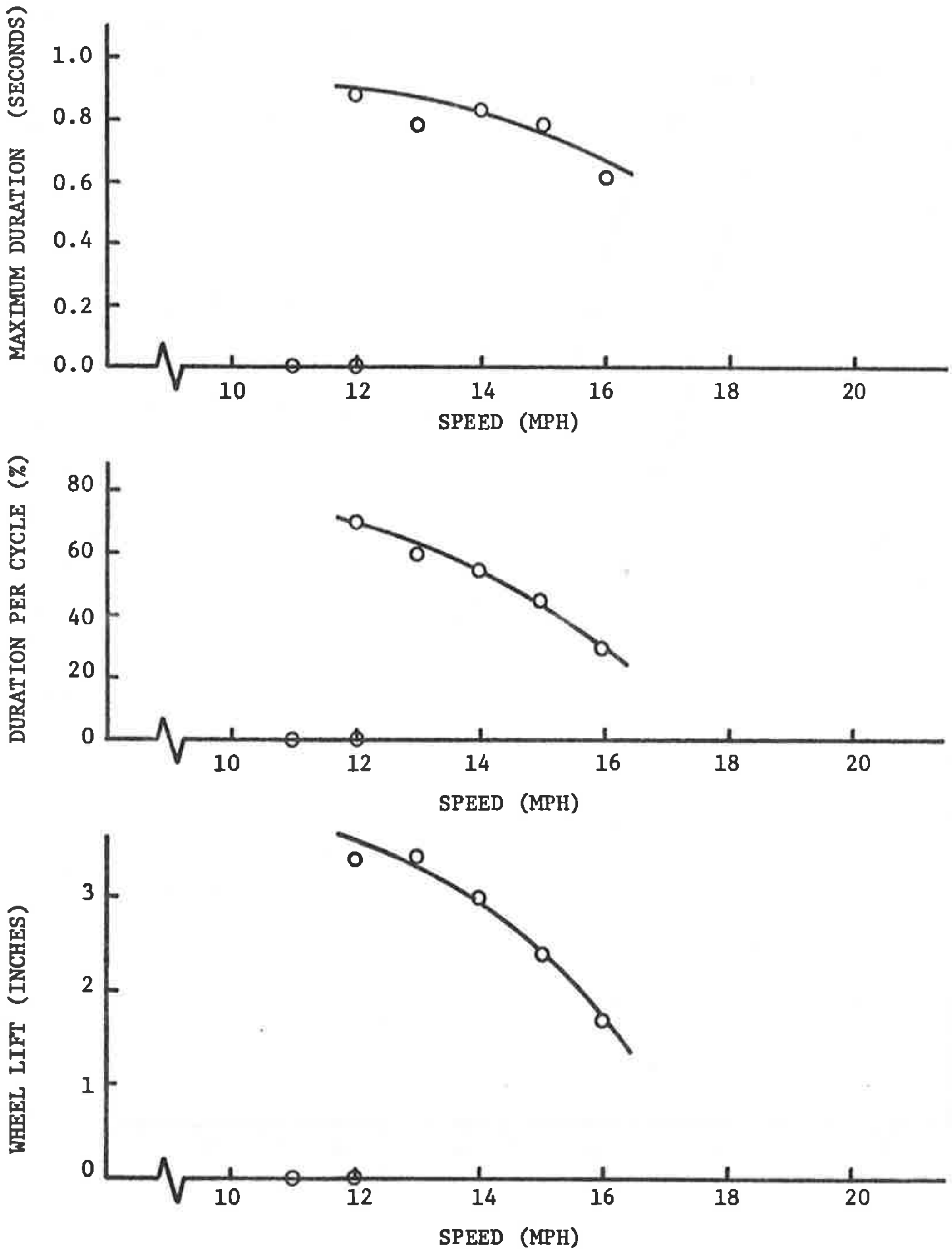

FIGURE 25. AMOUNT AND DURATION OF WHEEL LIFT FOR 100-TON CAR OBTAINED FROM RESPONSES TO 1-INCH RAIL CROSS LEVEL DIFFERENCE AT VARIOUS SPEEDS

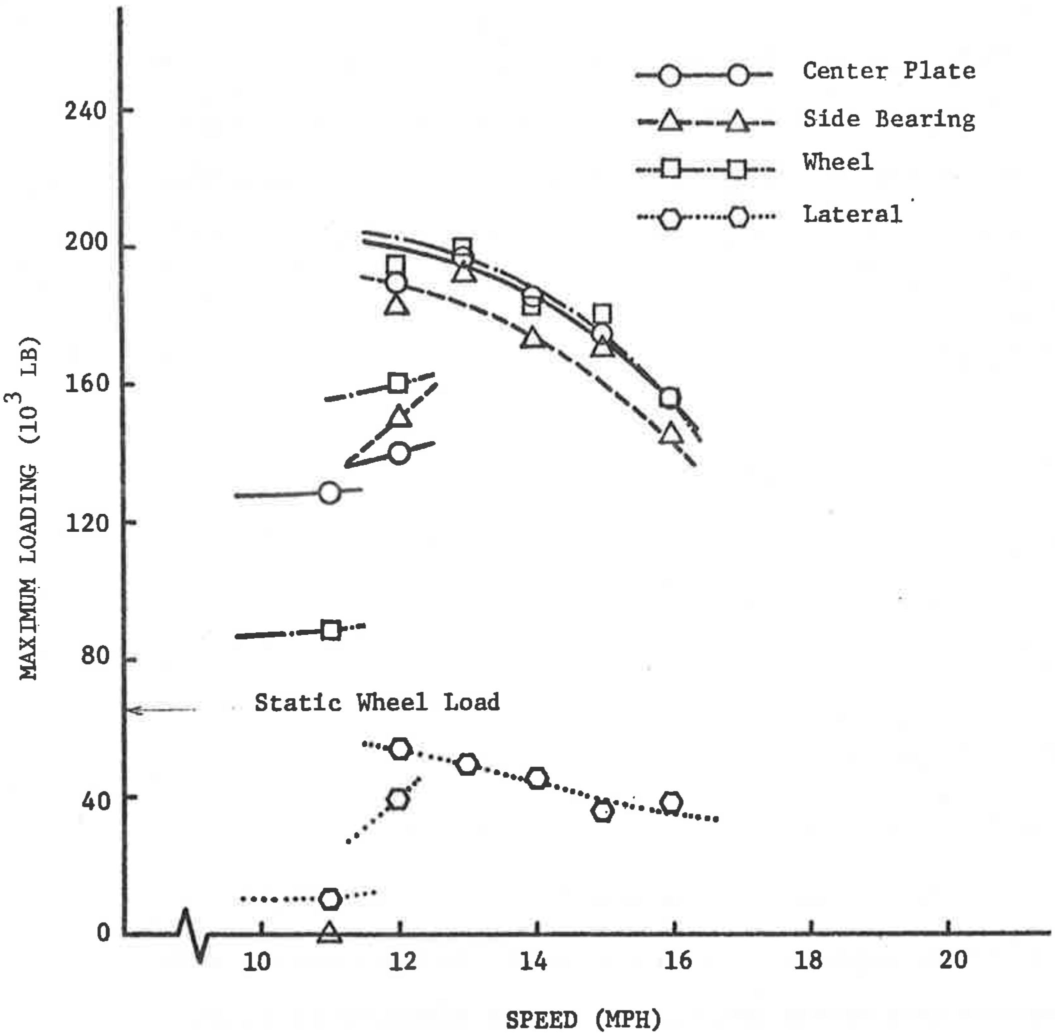

FIGURE 26. MAXIMUM LOADINGS FOR 100-TON CAR OBTAINED FROM RESPONSES TO 1-INCH RAIL CROSS LEVEL DIFFERENCE INPUT AT VARIOUS SPEEDS

forces significantly greater than static values occur under severe rocking conditions which approach 200,000 lbs for the 100 ton car in comparison to 110,000 lbs for the 70 ton car.

Finally to summarize the response data computed, Table 3 has been prepared which tabulates maximum roll angle, wheel lift, center plate, side bearing and wheel forces for a given car. The data shows that wheel force levels increase by a factor of 1.6 as the unloaded 70 ton car is loaded. They increase by 1.16 as a loaded 70 ton car passes from 0.75 to 1.0 track cross level amplitude. They increase by 1.67 as a loaded 70 car is replaced by a 100 ton loaded car running on a 0.75 inch cross level amplitude and by 1.11 as a loaded 100 ton car passes from 0.75 to 1.0 inch cross level amplitude. Because the rocking response is speed sensitive, these maximum force levels occur only near a critical speed and for operation at speeds lower than or higher than this critical speed force levels decrease by factors 2-3 and approch nominal static force levels.

3.3 Comparison of Response Data with Published Data

The digital simulation program described in this study, has been evaluated by comparing it with results of the AAR program. Roll angle response data versus speed for 70 ton car subjected to a 0.75 inch cross level amplitude are plotted in Figure 27 based upon the AAR computer program [4] and the program described in this report. The maximum roll angle responses for both simulations occur near 15 mph and are 6.8° for the AAR results and 7.2° for the reduced complexity program. A comparison of the maximum response values of wheel, side

TABLE 3

MAXIMUM RESPONSE VARIABLES AT SELECTED CAR SPEEDS

Condition	Speed	Roll Angle	Wheel Lift	Wheel Load	Side Bearing Load	Center Plate Load
	[mph]	[Degrees]	[in]	[lb]	[lb]	[lb]
Unloaded 70 ton car 0.75 inch cross level	33	3.2	1.9	60,000	54,000	62,000
Loaded 70 ton car 0.75 inch cross level	15.5	7.5	2.5	105,000	105,000	118,000
Loaded 70 ton car 1.0 inch cross level	15.0	9	2.7	120,000	118,000	120,000
Loaded 100 ton car 0.75 inch cross level	13	6.8	3.0	180,000	175,000	175,000
Loaded 100 ton car 1.0 inch cross level	13	7.8	3.3	200,000	200,000	200,000

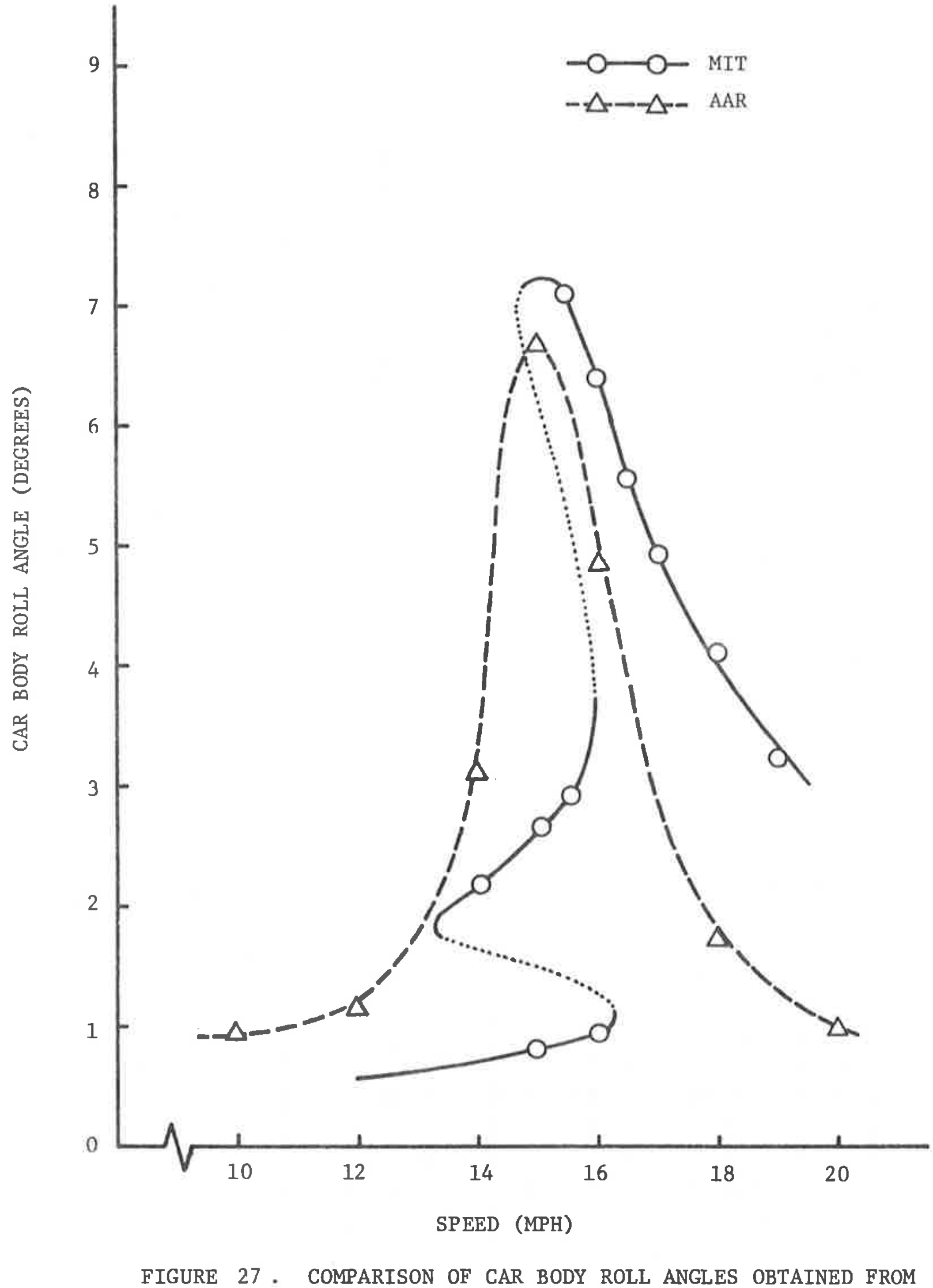

FIGURE 27. COMPARISON OF CAR BODY ROLL ANGLES OBTAINED FROM DIGITAL SIMULATIONS OF MIT AND AAR MODELS FOR 70-TON CAR WITH 0.75-INCH RAIL CROSS LEVEL DIFFERENCE INPUT AT VARIOUS SPEEDS

bearing and center plate forces at 15 mph is summarized in Table 4. The values of the forces agree within 15%. Thus relative good agreement is reached for the severe rocking condition. At other speeds while the general trends of the data for roll response are similar, a close one-to-one correspondence between points does not occur. While the program used in this study has shown multiple solutions exist depending upon initial conditions, the data plotted for the AAR program indicates only one data point for each speed. Because of the existence of multiple solutions to the rocking problem and the dependence of the maximum values plotted for each program upon initial conditions and upon duration of the run, it is difficult to directly compare solutions to two simulation programs without an extensive study in which both programs are run under precisely the same input and initial conditions.

The computation time requirements of the reduced complexity program are based upon running the program on an Interdata Model 80 Mini-Computer. For runs on this computer, the ratio of computer time to real time was less than 75. Thus, to run a 70 ton freight car time response for 15 seconds, 9 cycles of oscillation, requires about 19 minutes of computer time. At a cost of $45.00 per hour the cost for the run is about $15.00. The integration time step used in the simulation is 0.005 seconds.

Data for the AAR program indicate an integration time step of 0.00025 seconds is required for numerical stability [4]. This time step is a factor of twenty less than that for the reduced complexity program. This small time step is required so that the dynamic response

TABLE 4

COMPARISON OF 70 TON CAR RESPONSE
TO 0.75 INCH RAIL CROSS LEVEL
DIFFERENCE INPUT

Compared Output Variable	AAR Detailed Model	Reduced Complexity Model
Speed [mph]	15	15.5
Roll Angle [deg]	6.3	7.1
Wheel Force [10^3 lb]	100	119
Center Plate Force [10^3 lb]	110	102
Side Bearing Force (10^3 lb]	92	104

of the bolster mass on the gib stop spring (frequency ≃ 1000 hertz) may be computed accurately. Thus, the AAR program requires approximately 20 times the number of calculation steps per unit simulation time as the reduced complexity program. When the AAR program was run on an IBM-360-158, it had a computation to real time ratio of 100. On an IBM-370-158* the reduced complexity program is expected to have a computation to real time ratio of less than twelve. Thus, the reduced complexity model is expected to be a factor of at least eight times faster than the more detailed program.

---

*The IBM 370-158 computer is about five times faster than the Interdata Model 80 computer used in this study.

4. CAR STEADY-STATE RESPONSE USING A DESCRIBING FUNCTION TECHNIQUE

4.1 Freight Car Model

In addition to the direct digital simulation model, a describing function analysis has been performed to compute freight car response. This type of analysis yields the car body steady-state response to an equivalent sinusoidal cross level track input to the car. The method allows inclusion of the principal nonlinear effects of rail car motion though quasi-linearization techniques [11], yet employs linear frequency response techniques in its basic computations. The describing function analysis has been performed to determine the feasibility of applying describing function techniques to the freight car response pattern and in particular to determine if desired levels of response accuracy can be achieved with reduced computation time requirements in comparison to direct digital simulation methods. In this initial feasibility study the technique has been developed based upon the half car body freight car model illustrated in Figure 28.

In the model the wheelset is subjected to a sinusoidal cross level input, θ; transmitted through the rails which are modeled as very stiff nonlinear compression springs as shown in Figure 29. The wheelset has two degrees of freedom - a vertical translation, z_w, and a roll rotation, θ_w. It is free to rotate for small angles about either rail, thus providing a lateral wheelset displacement y_w. The suspension group is modeled as two parallel linear spring - nonlinear coulomb damper combination. The bolster has two degrees of freedom, a vertical transla-

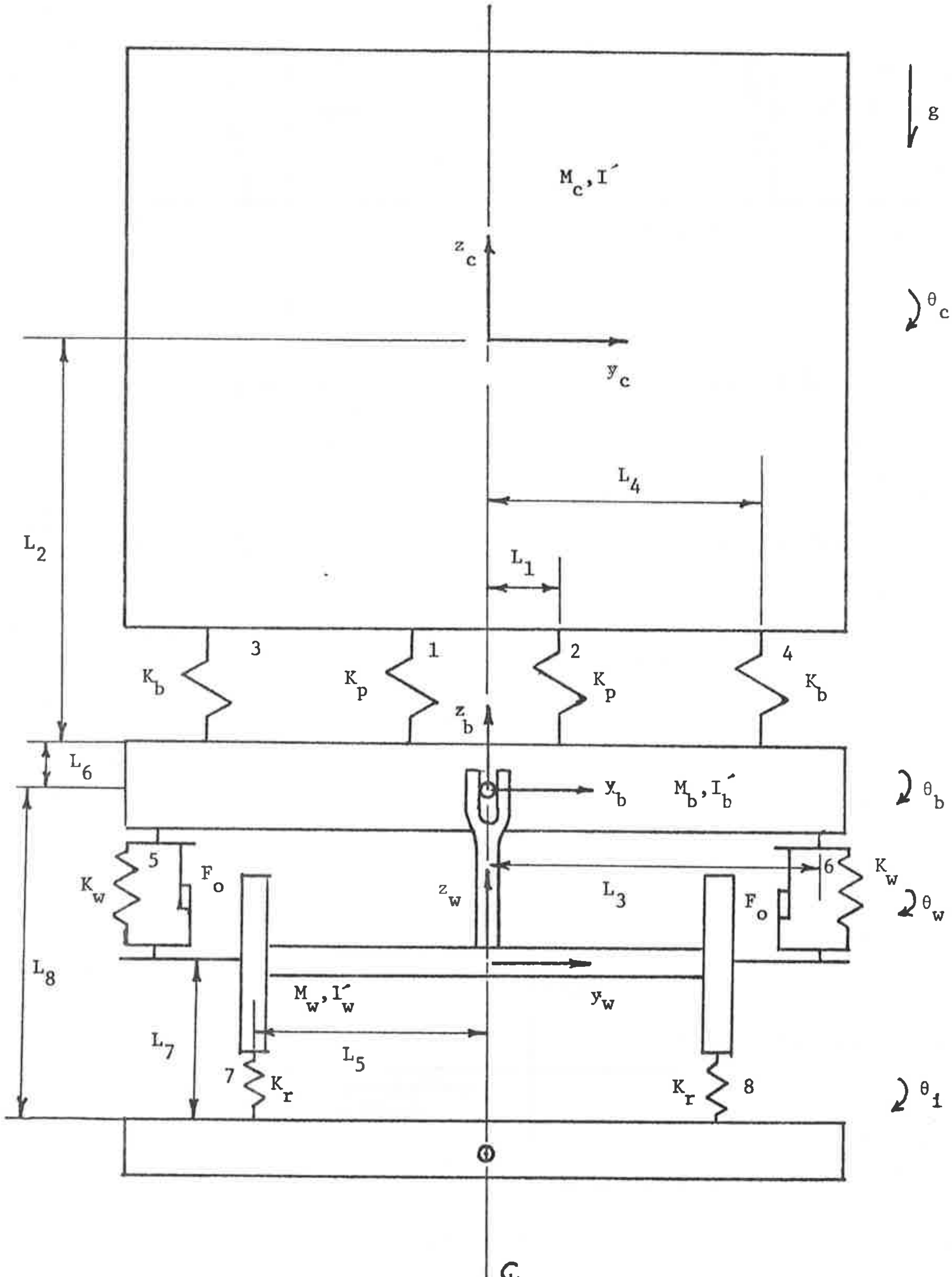

FIGURE 28. CONSTITUTIVE MODEL

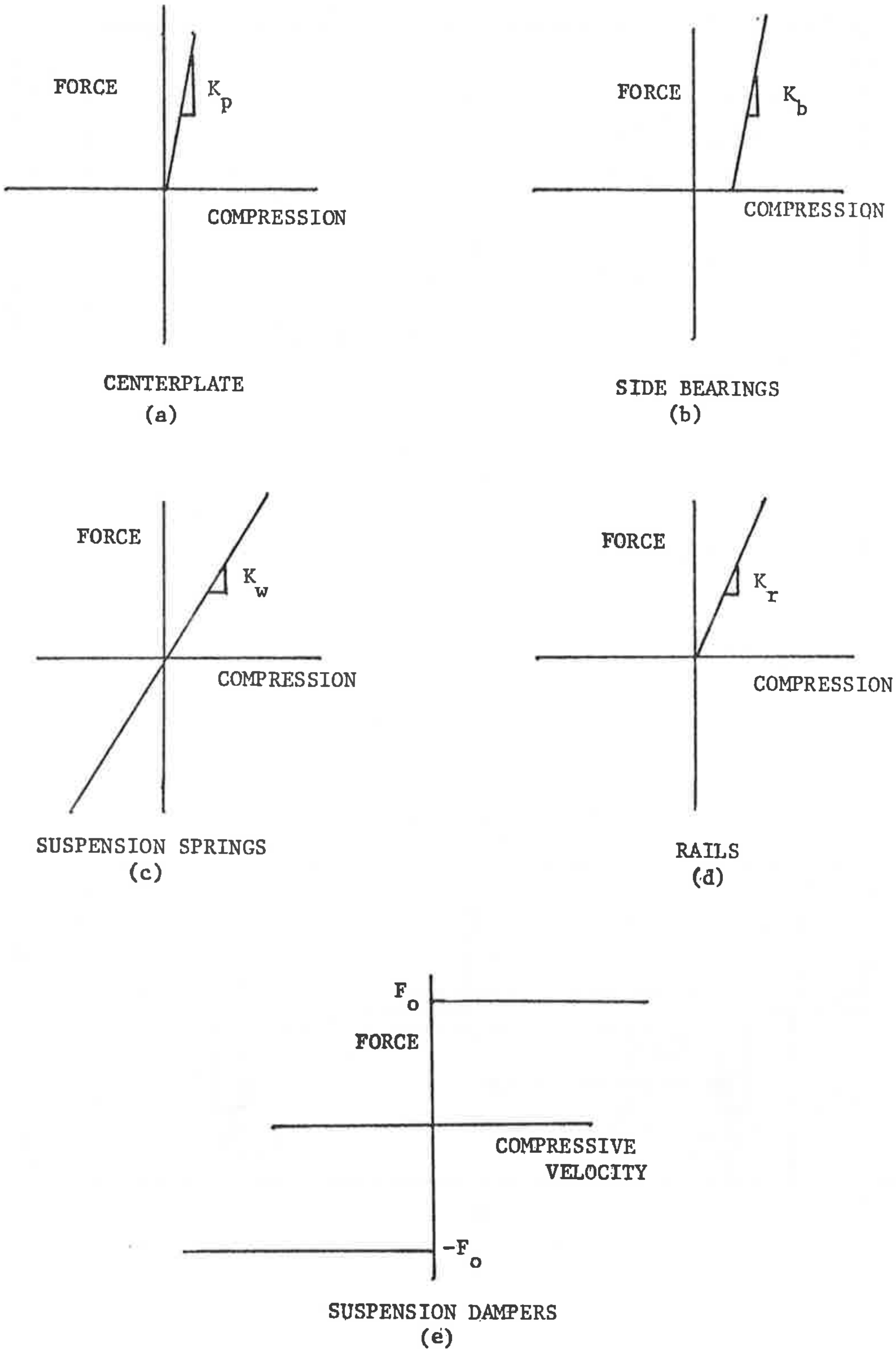

FIGURE 29. CONSTITUTIVE RELATIONS

tion, z_b, and a roll rotation, θ_b. Small lateral bolster excursions, y_b, are allowed as the wheelset and bolster rotate through small angles about the rails. The lateral motion is governed by small displacements and is dependent on the angular rotations. The centerplate is modeled as a pair of very stiff nonlinear compression springs whose characteristics are shown in Figure 29. The stiffness of the springs is the elasticity of the centerplate material. The side bearings are also modeled as a pair of very stiff nonlinear compression springs with a threshold to represent nominal clearance between the car body and bolster. The side bearing nonlinear spring representation is shown in Figure 29. The car body has two degrees of freedom - the vertical translation, z_c, and the roll rotation, θ_c. Small lateral displacements, y_c, can occur by the car body rocking on either the center plate or the side bearings.

This 1/2 car body model has six degrees of freedom and various nonlinear representations to model wheel lift, coulomb friction, center plate rocking, and side bearing rocking.

The equations describing the half car body motion may be derived directly from force and moment balance conditions as well as kinematic constraints. The vertical force balance equations on the car body, bolster, and wheelset are:

$$M_c \ddot{z}_c = F_1 + F_2 + F_3 + F_4 - M_c g \qquad (11)$$

$$M_b \ddot{z}_b = F_5 + F_6 - F_1 - F_2 - F_3 - F_4 - M_b g \qquad (12)$$

$$M_w \ddot{z}_w = F_7 + F_8 - F_5 - F_6 - M_w g \, , \qquad (13)$$

where F_1 through F_8 are the forces acting at points 1 through 8 in Figure 28 and are the nonlinear spring forces defined in Figure 29.

The moment balance equations are:

$$I_c' \ddot{\theta}_c + \ell_2 F_{y_c} = \ell_1(F_2 - F_1) - \ell_4(F_4 - F_3)$$

$$I_b' \ddot{\theta}_b + \ell_6 F_{y_b} = \ell_1(F_1 - F_2) + \ell_4(F_4 - F_3) - \ell_3(F_6 - F_5)$$

$$I_w' \ddot{\theta}_w + \ell_8 F_{y_w} = \ell_3(F_6 - F_5) - \ell_5(F_8 - F_7)$$

where the forces F_{y_c}, F_{y_b}, and F_{y_w} are the lateral forces exerted on the car body, bolster and wheelset respectively. If it is assumed that the angles of rotation are small and that no relative lateral motion can occur between the bolster and wheelset the following kinematic constraints exist:

$$y_c \approx \ell_2\theta_c + \ell_6\theta_b + y_b$$

$$y_b \approx \ell_8\theta_w$$

$$y_w \approx \ell_7\theta_w$$

using these relationships in the moment balance equations yields:

$$I_c \ddot{\theta}_c + M_c \ell_2\ell_8 \ddot{\theta}_w + M_c \ell_2\ell_6 \ddot{\theta}_B = - \ell_1(F_2 - F_1) - \ell_4(F_4 - F_3) \quad (14)$$

$$I_b \ddot{\theta}_B + M_c \ell_2\ell_6 \ddot{\theta}_c + M_c \ell_8\ell_6 \ddot{\theta}_w = \ell_1(F_1 - F_2) + \ell_4(F_4 - F_3) + \ell_3(F_6 - F_5) \quad (15)$$

$$I_w \ddot{\theta}_w + M_c \ell_2\ell_8 \ddot{\theta}_c + M_c \ell_6\ell_8 \ddot{\theta}_B = \ell_3(F_6 - F_5) - \ell_5(F_8 - F_7). \quad (16)$$

The track input to the dynamic equations occurs through F_7 and F_8 which are functions of $\ell_5(\theta_w - \theta_i)$ where θ_i is the track angular displacement.

The inertias in the equations summarized above can be expressed as:

$$I_c = I_c' + M_c \ell_2^2$$

$$I_b = I_b' + M_c \ell_6^2$$

$$I_w = I_w' + M_w \ell_7^2 + (M_c + M_b)\, \ell_8^2 ,$$

where: I_c', I_b' I_w' refer respectively to inertias referenced respectively to the car body, bolster and wheelset center of mass.

The six dynamic equations (11) - (20) and the force-relative displacement and force relative velocity constitutive relations represent a nonlinear description of the half car body model. These equations may be summarized after some manipulation in the form:

$$\underline{\ddot{X}} = \underline{G}(\underline{X},\ \underline{\dot{X}},\ \theta_i(t)) \tag{17}$$

where: $\underline{X}$ vector of six position vairables which describe the car-body, bolster and wheelset:

$$\underline{X} = \begin{bmatrix} z_c \\ \theta_c \\ z_B \\ \theta_B \\ z_w \\ \theta_w \end{bmatrix},$$

where $\theta_i(t)$ is the track input effective rotation.

and where the function $\underline{G}$ represents the nonlinear dynamic equations represented by (11)-(16) with the nonlinear spring and damper constitutive relationships included directly.

The model summarized in (17) includes the bolster and wheelset masses and inertias and is similar to the AAR detailed model in treatement of the rail, center plate and side bearings stiff springs. In the describing function technique, because direct numerical integration of the equations is not used for solution, a strong penalty in computer time requirements is not incurred with the inclusion of these high frequency effects. The model includes the principal nonlinear effects associated with wheel lift, center plate separation and side bearing contact. Coulomb damping effects are also included. Because the model is a basis for an initial feasibility study of limited scope, hardening of the suspension springs has been neglected and the bolster has been assumed to have no lateral motion with respect to the track.* The model contains a sufficient number of the fundamental types of freight car nonlinearities to serve as a good test of the describing function technique.

4.2 The Describing Function Solution Technique

The describing function technique yields the steady-state sinusoidal response of a nonlinear system when the system is subjected to an input sinusoidal function. In the technique it is assumed that the track cross level input, rotation $\theta_i(t)$ may be represent as:

$$\theta_i(t) = A \sin\omega t \ , \tag{18}$$

where: A = amplitude

ω = frequency

---

*The model may be readily extended to allow suspension spring hardening and lateral bolster movement.

With the input (18), it is assumed that each position variable X_i in the position vector $\underline{X}$ is also sinusoidal in form and may be represented as:

$$X_i = a_{oi} + \sum_{n=1}^{\infty} a_{ai} \sin n\omega t + \sum_{n=1}^{\infty} b_{ni} \cos n\omega t \ . \qquad (19)$$

In the analysis, the primary motivation for using the describing function technique is that the Fourier series provides a good approximation to the response variables when only a few terms are used.* The response time histories in Chapter 3 exhibit frequency components which have a constant level (a_o), a first harmonic (a_1, b_1) and a second harmonic (a_2, b_2), the second harmonic is especially visible in the vertical motion of the car body. In the work below each of the position variables X_i is represented as:

$$X_i(t) \approx a_{oi} + a_{1i}\cos(\omega t) + b_{1i}\sin(\omega t) + a_{2i}\cos(2\omega t) + b_{2i}\sin(2\omega t) \ . \qquad (20)$$

Combinations of these position variables reduce to the relative displacements which determine the forces generated in the nonlinear spring elements in the model.

Since all of the nonlinear forces are piecewise linear, a representative force $F_i(t)$ can be represented in terms of a Fourier series with the first two harmonics:

$$F_i(t) \simeq F_{oi} + C_{1i}\cos(\omega t) + D_{1i}\sin(\omega t) + C_{2i}\cos(2\omega t) + D_{2i}\sin(2\omega t) \ . \qquad (21)$$

*If the model were linear, only one term n=1 is required.

The coefficients of the truncated Fourier series can be found by the standard Fourier integrals, i.e.,

$$F_{oi} = \frac{1}{2\pi} \int_{o}^{2\pi} F_i(\omega t)\ d(\omega t)$$

$$C_{1i} = \frac{1}{\pi} \int_{o}^{2\pi} F_i(\omega t)\ \cos(\omega t)\ d(\omega t)$$

$$D_{1i} = \frac{1}{\pi} \int_{o}^{2\pi} F_i(\omega t)\ \sin(\omega t)\ d(\omega t)$$

$$C_{2i} = \frac{1}{\pi} \int_{o}^{2\pi} F_i(\omega t)\ \cos(2\omega t)\ d(\omega t)$$

$$D_{2i} = \frac{1}{\pi} \int_{o}^{2\pi} F_i(\omega t)\ \sin(2\omega t)\ d(\omega t)\ . \qquad (22)$$

Since $F_i(t)$ is a piecewise linear function the above integrals can be computed in closed form.

The substitution of the position variables and nonlinear forces expressed as equations (20) and (21) into equations (17) results in a series of algebraic equations by equating the constant first harmonic, and second harmonic terms of the Fourier series for each variables.

These algebraic equations may be summarized as:

$$\underline{G}_o = 0$$

$$\underline{G}_1 = -\ \omega^2 \underline{X}_1$$

$$\underline{G}_2 = -(2\omega)^2 \underline{X}_2\ , \qquad (23)$$

where $\underline{X}_1$ and $\underline{X}_2$ represent the first and second harmonic components of the position vector $\underline{X}$ and $\underline{G}_o$, $\underline{G}_1$, and $\underline{G}_2$ are the average value, and the first and second harmonic components of the function $\underline{G}$. These equations are a set of nonlinear algebraic equations which may be solved using conventional search algorithms. Equation (23) represents thirty coupled, nonlinear algebraic equations. However, by expressing the equations in scalar form and using the fact that all of the nonlinearities occur in symmetric pairs about the vertical centerline, the number of scalar equations can be reduced to fifteen. The fifteen independent scalar equations require the first three Fourier coefficients for each force. All of the nonlinearities are piecewise linear hence, the required integrations to compute the Fourier coefficients can be performed analytically once the zero crossings are known. Thus, the solution of the freight car steady state rock and roll response to sinusoidal cross level inputs involves two major subtasks:

a. Evaluation of appropriate Fourier coefficients for the nonlinear forces.

b. Solution of a set of fifteen nonlinear algebraic equations.

A flow chart of the computer algorithm developed to accomplish these two tasks is summarized in Fig. 30.

In the algorithm an initial estimate of the Fourier amplitude coefficients of the position vector X is made, the forces corresponding to these amplitudes are computed and then the algebraic equations are evaluated to determine if they are satisfied. A root solving algorithm developed by Powell [12] was used to determine this solution. As shown in Fig. 30, the solution process is iterative. The solution yields

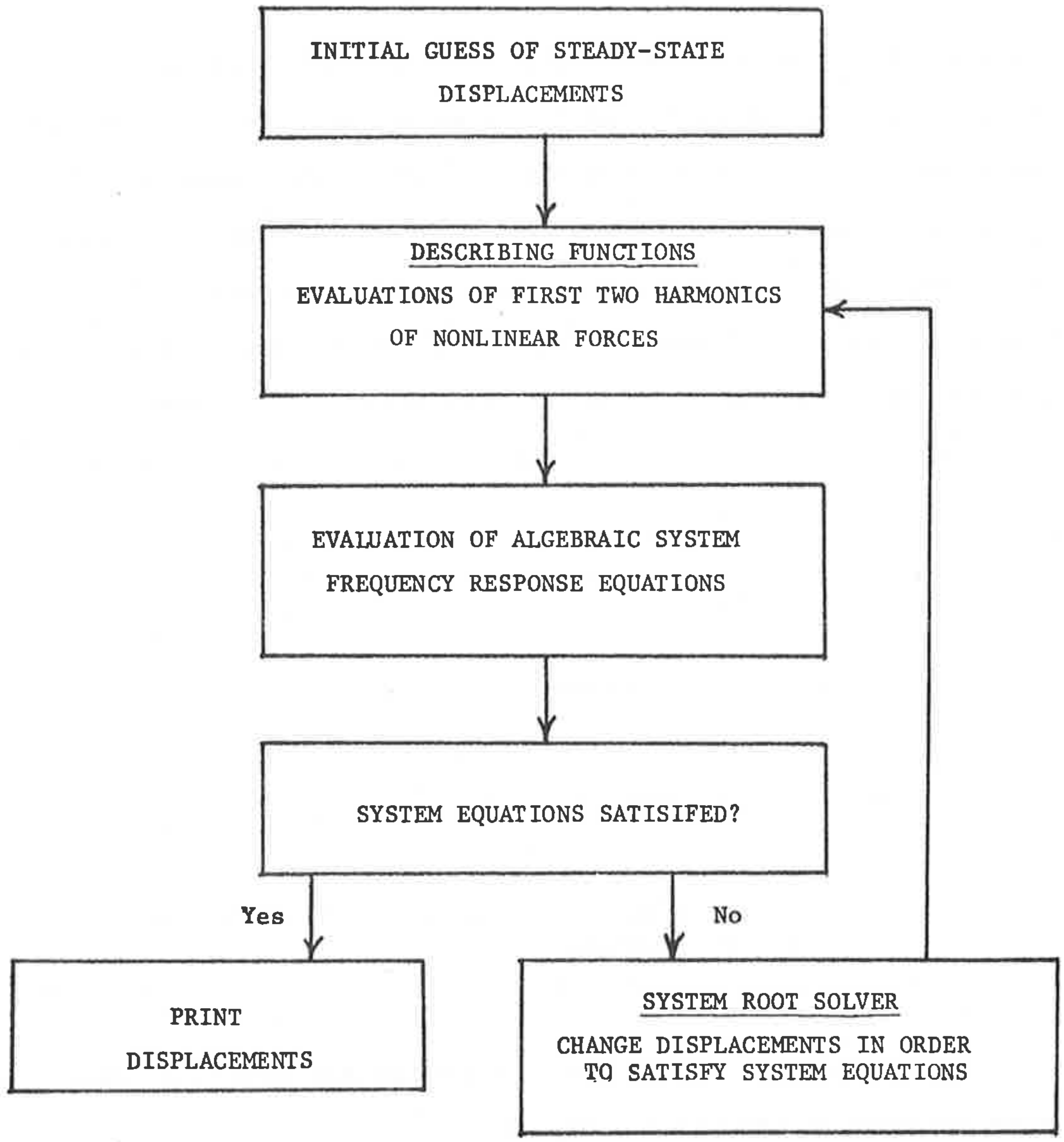

FIGURE 30. DESCRIBING FUNCTION ALGORITHM

then, the displacements and forces which in steady-state satisfy the equation of motions. When an initial input frequency corresponding to car velocity V is considered, the search, process for a solution may be quite lengthy, however, after one solution is obtained, the initial estimate of position variables for a new increased or decreased frequency (i.e., an increase or decrease in speed) solution may be based upon the previous solution and a set of solutions for different speeds may be obtained efficiently. When a good first estimate of the position vector is used, the solution to the equations for the half car body model may be obtained in less than 30 secs. of Interdata M80 computer time. Thus, the describing function technique is efficient for parametric studies, in which once a solution is found, it is desired to change a system parameter incrementally and generate a set of solutions.

4.3 Steady-State Response Data

The describing function analyses has been used to determine steady-state response amplitudes for the 70 ton car. Response data illustrating roll angle amplitude as a function of car forward velocity are summarized in Fig. 31 for three levels of track cross level amplitude. The data illustrate that for all three cross level amplitudes multiple solutions exist for the same operating speed. The solid lines represent stable operating points while the dashed lines represent unstable operating points. Which stable solution is obtained depends upon the initial conditions of the car. As car speed is increased from 12 mph the solutions follow the lower curves until a speed of 16 mph, 17 mph and 19.5 mph are reached respectively for the 0.5, 0.75 and 1.0 inch amplitude inputs.

At these speeds the response suddenly jumps up to the next stable curve follows this curve and then jumps up the next set of curves. As speed is increased further the amplitude decreases when operating on the highest set of curves. For the 0.5 inch amplitude a very small speed range exists 19.5-20 mph for which the response can jump up to the highest set of curves for increasing speed.* As speed is decreased from 20 mph, the response is given by the highest set of curves which extend to 12 mph. Whether a car response will achieve the high levels of response shown, i.e., $\pm$ 10° at 12 mph depends on its initial conditions and whether a sufficiently long section of track is available to build the response up to these steady-state levels.

The duration of wheel lift is plotted in Fig. 32. Wheel lift was only found to occur for the high amplitude level response curve displayed in Fig. 31. When operating at this high amplitude response level, the wheel lift duration per cycle approaches 50% for the 10-16 mph speed range and decreases as speed is increased to 20 mph to 10% per cycle.

The wheel vertical and lateral force for the 70 ton amplitude response are plotted in Fig. 33. The vertical forces reach amplitudes that increase from 90,000 lbs at 18 mph to 140,000 lb at 12 mph for the high amplitude response. These dynamic force levels range from 2 to almost 3 times the static force levels.

Finally in Fig. 34, the response computed with the describing function and digital simulation programs are compared. Both analyses

---

*This speed window shown in the steady-state response data for the 0.5 inch input data could not be penetrated when direct digital simulation results were obtained, thus in Fig. 17, the highest curve was not obtained for the 0.5 inch input amplitude.

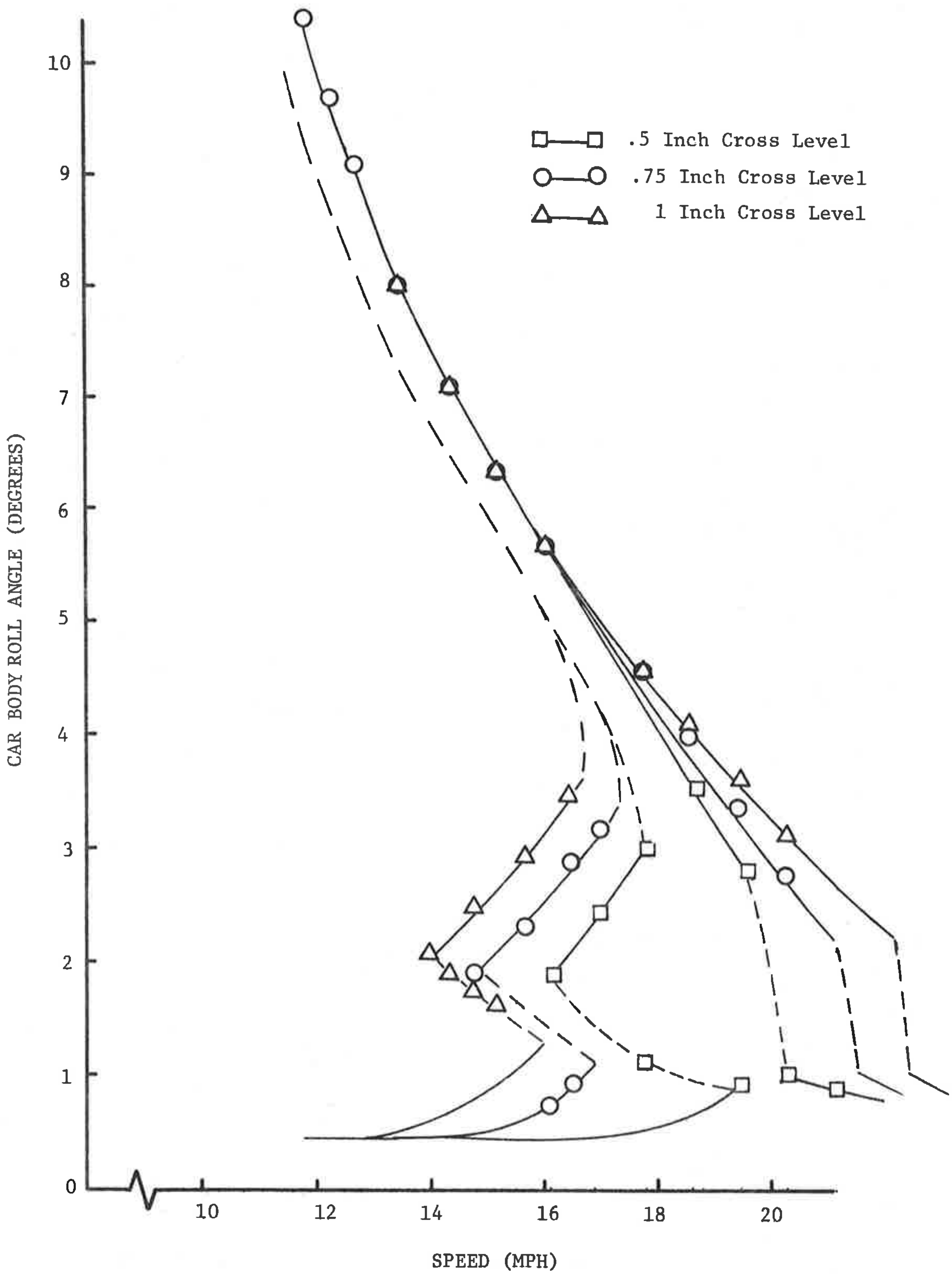

FIGURE 31. CAR BODY ROLL ANGLE FOR 70-TON CAR OBTAINED FROM A DESCRIBING FUNCTION ANALYSIS

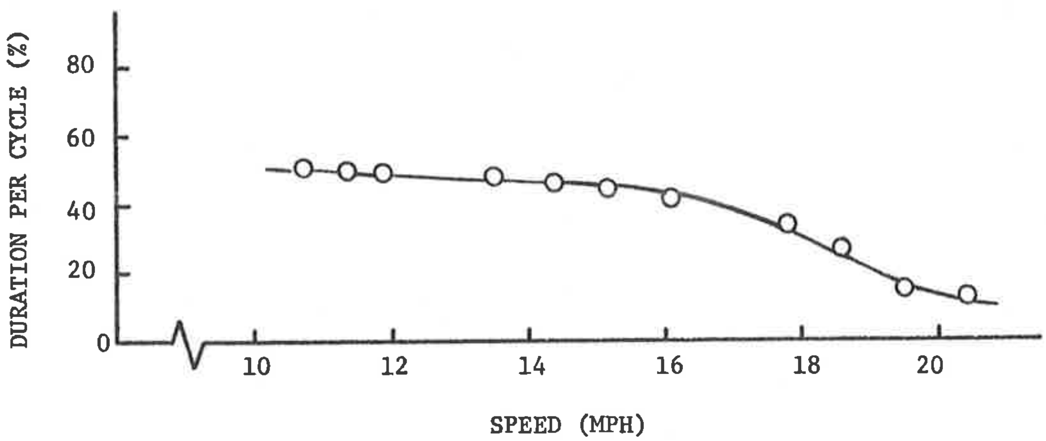

FIGURE 32. DURATION OF WHEEL LIFT FOR-70 TON CAR OBTAINED FROM A DESCRIBING FUNCTION ANALYSIS FOR 0.75-INCH CROSS LEVEL INPUT

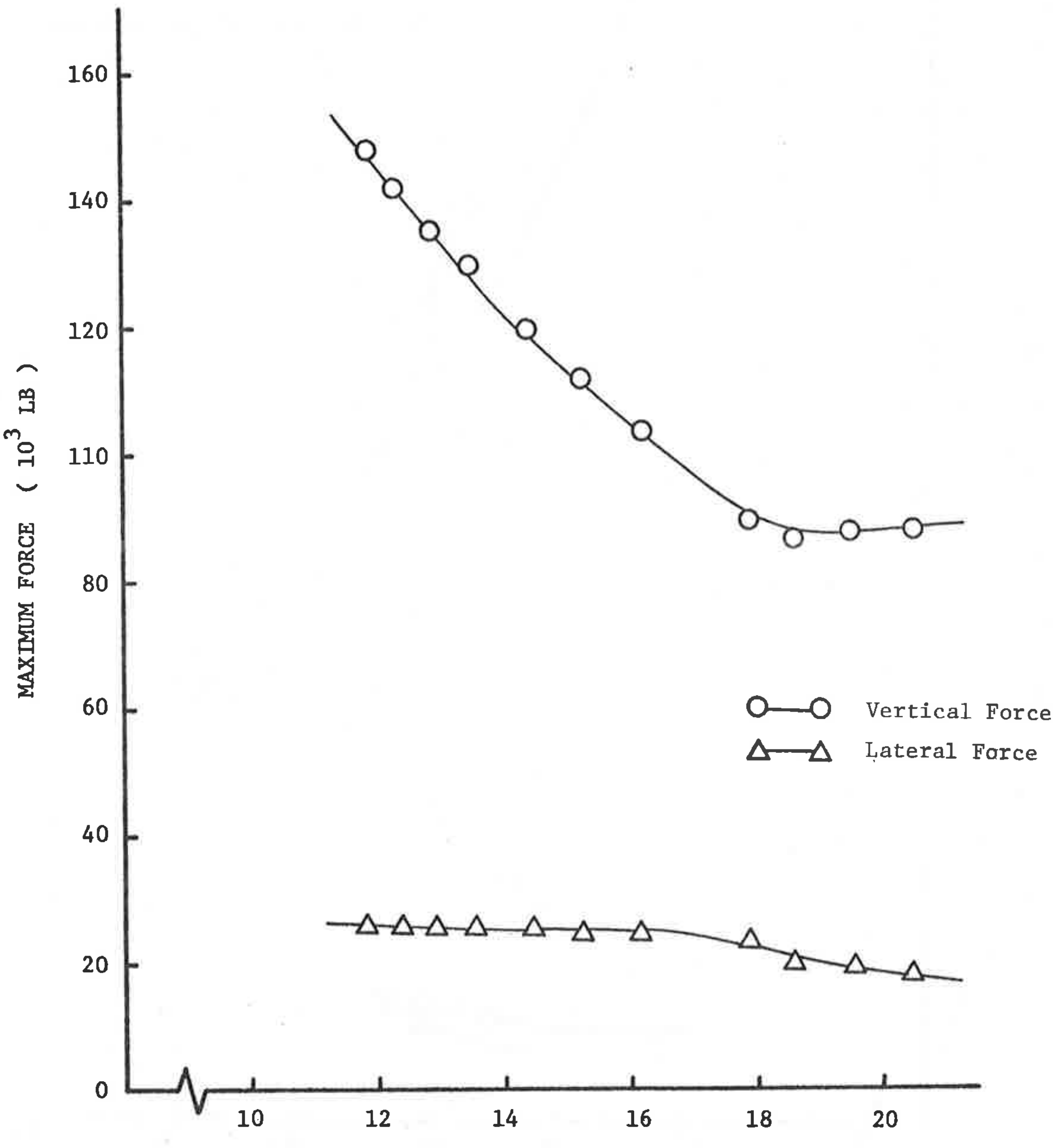

FIGURE 33 . MAXIMUM FORCES FOR A 70-TON CAR OBTAINED FROM A DESCRIBING FUNCTION ANALYSIS WITH 0.75-INCH CROSS LEVEL INPUT

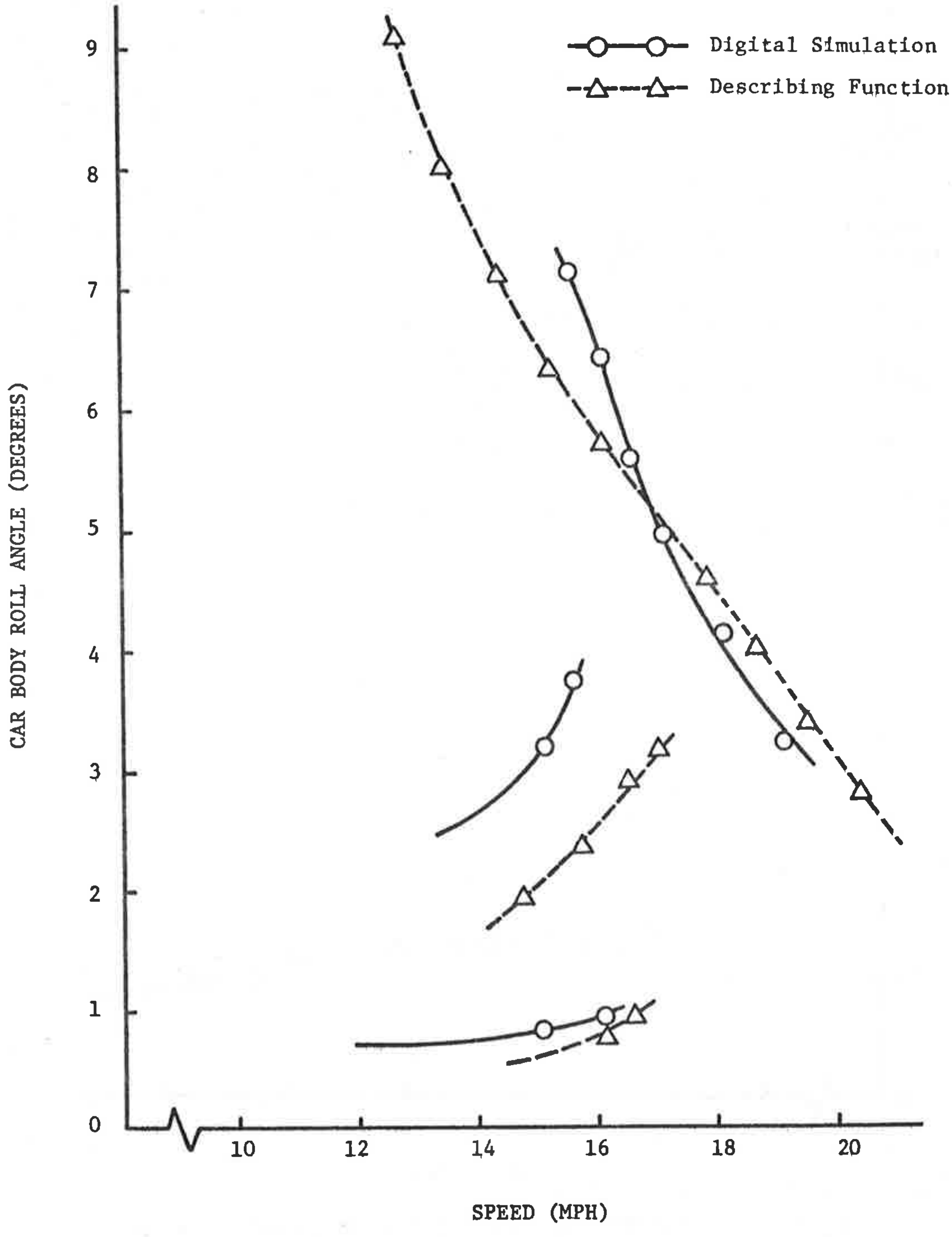

FIGURE 34 . COMPARISON OF CAR BODY ROLL ANGLES OBTAINED FROM DIGITAL SIMULATION AND DESCRIBING FUNCTION ANALYSIS FOR 70-TON CAR WITH 0.75-INCH RAIL CROSS LEVEL DIFFERENCE INPUT AT VARIOUS SPEEDS

demonstrate the existence of multiple solutions and the lowest and highest amplitude levels of response agree closely, while the intermediate response level curves differ by 30%. The describing function analysis demonstrates the existence of higher levels of steady-state response than were achieved with the digital simulation program. For speeds below 16 mph, digital simulation program solutions could not be obtained for the highest level of response curve. For all the initial condition values tried, the solution always tended to the lower amplitude level responses. The describing function model also differs in a number of respects from the digital simulation model, primary in its use of linear suspension springs (nonhardening) and neglect of lateral bolster motion. Both of these effects tend to allow higher levels of rocking amplitude and lead to existence of a higher range of rocking amplitudes solutions.

In summary, the feasibility of using describing functions for computation of rail car rocking response has been demonstrated. The technique provides an efficient method of generating parametric response data.

5. CONCLUSIONS AND RECOMMENDATIONS

In this study a reduced complexity digital simulation program and a quasi-linear describing function program have been evaluated for computation of freight car rocking response to track cross level variations. The reduced complexity digital simulation neglects the high frequency dynamic response of bolster and wheelset masses but includes fundamental nonlinearities associated with center plate separation, side bearing contact, wheel lift, spring bottoming and coulomb friction. This model permits calculation of the car response time history to track cross level variations in less than one eighth the time required of more detailed simulation programs which inlcude high frequency behavior associated with the bolster and wheelset masses. Comparison of the response predictions of this program with the AAR simulation program for a 70 ton car response to 0.75 inch cross level variation at maximum roll response indicated that the two programs predicted roll angle, center plate force, side bearing force and wheel force within 15%.

A study of a quasi-linear describing function technique, which generates the steady-state car response from a set of nonlinear algebraic equations, has demonstrated the basic feasibility of the technique for the types of nonlinearities characterizing freight car dynamics. The procedure is particularly effective for parametric studies, since once a solution is obtained for one set of parameter values, additional solutions for incremental changes in a parameter value can be obtained efficiently. It is estimated that incremental types of solutions can be generated using 30 sec of Interdata M 80 computer time per solution for a half car body model.

Parametric studies of 70 and 100 ton freight cars have been conducted for 0.5, 0.75 and 1.0 inch track cross level variations. These studies have shown that for the 0.75 and 1.0 inch amplitude irregularities severe rocking conditions with rocking angles of greater than $\pm$ 7° and wheel lift in excess of 1.5 inch with a duration approaching 50% of a rocking cycle occurs for a loaded 70 car in the 14-16 mph range and for the loaded 100 ton car in the 12-15 mph range. Under these severe rocking conditions wheel forces which approach 2-3 times nominal static force levels occur.

The study has also shown that because of the nonlinear effects in rail car response associated with rocking off the center plate to the side bearings several types of response behavior, i.e., light, moderate or severe rocking may occur for a given set of car and track parameters at a specific operating speed. Which response regime occurs depends upon the initial conditions of the car just prior to its entering the current operating condition, i.e., on whether the car is approaching the operating condition from a higher or lower speed. The data in this study shows that under severe rocking conditions higher force levels are obtained as the car approaches a condition by slowing down, i.e., from a higher speed. Under these conditions gradually decreasing the speed of train operation can lead to increased rocking rather than reduced rocking until the speed is reduced below the point of a severe rocking condition. These effects are due to the nonlinear jump response type of response which results from the nonlinear center plate side bearing restoring forces.

In conclusion, this study has shown the merit of reduced complexity digital simulation models and quasi-linear describing function techniques for parametric studies of freight car response. These programs have reduced computer time requirements in comparison to more detailed simulation models. These programs merit consideration for studies of car transient and steady-state operating characteristics and for trade-off studies to determine preliminary effects of design changes. For detailed design studies in which bolster and wheelset detailed transient response data are required, the more complex simulation programs are more appropriate.

6. REFERENCES

1. Weibe, D., "The Effects of Lateral Instability of High Center of Gravity Cars," ASME Trans. Vol. 90-B, No. 4, p. 462, November 1968.

2. Liepins, A.A., "Digital Computer Simulation of Railroad Freight Car Rocking," Trans. ASME, Journal of Engineering for Industry, Vol. 90, Series B, No. 4, p. 701-707, 1968.

3. Manos, W.P. and J.C. Shang, "Dynamic Analyses of Rolling Freight Cars," ASME Paper 6-5WA/RR-8, 1965.

4. Tse, Y.H., and G.C. Martin, "User's Manual, Flexible Body Railroad Freight Car," AAR Publication, 1975.

5. Tse, Y.H., "Methods of Analyses for the Dynamic Behavior of a Flexible Body Railroad Freight Car," M.S. Thesis, Department of Mechanical Engineering, Illinois Institute of Technology, December 1974.

6. Shum, K.L. and T. Willis, "A Mathematical-Computer Simulation of the Dynamics of a Freight Element in a Railroad Freight Car," Report IIT-Trans-75-2, Illinois Institute of Technology, 1975.

7. Healy, M.J., "A Computer Method for Calculating Dynamic Responses of Nonlinear Flexible Rail Vehicles," Wyle Laboratories Report, 1976.

8. "Computer Simulation of the Response of 70 Ton Box Cars," A Stucki Company Report, Pittsburgh PA, 1970.

9. Platin, B., "Dynamic Analyses and Stabilization Control of Freight Car Rocking," Sc.D. Thesis in Progress, Department of Mechanical Engineering, Massachusetts Institute of Technology (1977).

10. Emerson, G., "Freight Car Rocking Dynamics Using Analog Simulations," S.B. Thesis, Department of Mechanical Engineering, Massachusetts Institute of Technology, 1975.

11. Gelb, A. and W. VanderVelde, Multiple-Input Describing Functions and Nonlinear System Design, McGraw-Hill, New York NY, 1968, p. 655.

12. Rabinowitz, P., Numerical Methods for Nonlinear Algebraic Equations, Gordon and Breach Science Publishers, London, England, 1970, p. 115.

7. APPENDIX

The material presented in this report has been thoroughly reviewed and does not contain patentable or copyrightable material. The innovations reported in this document are described in Section 2 and Section 4 concerning computational techniques efficiently to compute the response of a freight car to sinusoidal track cross-level inputs.